

# HIE-ISOLDE, the project and the physics opportunities<sup>\*</sup>

M.J.G. Borge<sup>1,2,a</sup> and K. Riisager<sup>3</sup>

<sup>1</sup> ISOLDE, EP Department, CERN, CH-1211 Geneva 23, Switzerland

<sup>2</sup> Instituto de Estructura de la Materia, CSIC, E-28006 Madrid, Spain

<sup>3</sup> Department of Physics and Astronomy, Aarhus University, DK-8000 Aarhus C, Denmark

Received: 5 July 2016 / Revised: 11 September 2016

Published online: 17 November 2016 – © Società Italiana di Fisica / Springer-Verlag 2016

Communicated by N. Alamanos

**Abstract.** The ISOLDE facility at CERN offers the largest selection of ISOL beams today. The overall aim of the HIE-ISOLDE project is to enlarge the physics domains achievable with these beams, in particular by raising the maximum energy of post-accelerated beams to more than 10 MeV/u. An outline of the history of the project is followed by a succinct description of the superconducting linac chosen for acceleration and an overview of the parts of the project aiming to the improvement of the beam quality and intensity. Concrete examples are given of experiments that will be performed at HIE-ISOLDE.

## 1 Introduction

Now that HIE-ISOLDE is delivering its first results, it is the appropriate time for summarising the whole project. It is part of the world-wide effort during the last decades to improve upon radioactive beams, a branch of nuclear structure physics that during the last decades has moved from being a speciality subject to being the mainstream. This dramatic move has been triggered by the observation of significant changes in nuclear structure [1] as one goes away from the stable nuclei towards the neutron (and proton) driplines, but it is of course also driven by substantial technical progress that has provided experiments with radioactive beams of sufficient quality.

One is still far from having an ideal facility where one could “dial an isotope” of arbitrary neutron and proton numbers  $N$  and  $Z$  and have a beam delivered with intensities and properties approaching that obtainable for stable isotopes. There are two major processes for the production of radioactive beams: the in-flight and the ISOL (Isotope separator on-line) methods. In the former process the primary beam is fragmented passing through a thin target and the secondary products are produced in-flight, in the latter the primary beam interacts with a thick target and the secondary products stopped into the target are ionised and extracted. Due to decreasing production cross-sections in both cases there is a rapid decrease in secondary beam intensity as we approach more exotic nuclei. Also the limited target thickness necessary for transmit-

ting the secondary products is a limiting factor for the in-flight method. In the ISOL method the stopped fragments are thermally extracted, a process which introduces an extra delay strongly limiting the intensity of shortly living nuclei. See, *e.g.* [2], for a recent review. The two methods naturally lead to high and low energies of the radioactive ion beam, RIB, respectively, but many beam manipulation procedures have been developed and are used extensively to cover as large an energy range as possible. Still, the region of RIB of a few MeV/u up to a few tens of MeV/u has been the last to be explored. A major aim for HIE-ISOLDE has been to increase the energies of the existing reaccelerated beams from the ISOLDE facility at CERN to cover better this range.

This paper focuses on the HIE-ISOLDE project, mainly on the energy and intensity upgrades but addresses also additional requirements important for experimentalist. The purity of the beam (the level of contaminants) is often a crucial factor, but depending on the experiments, the beam optical properties, its time structure, its energy definition or the flexibility of changing the energy can also be important.

The HIE-ISOLDE initiative therefore included intensity upgrades as well as improvements of the beam quality, the latter to be understood in a quite general sense. As we shall discuss the different parts of the project take place on different timescales, the beam quality improvements are implemented continuously, the energy upgrade is now giving the first physics results, whereas a major part of the intensity upgrade is still to come.

We start in sect. 2 giving an overview of the history of HIE-ISOLDE from the first ideas to the completion of stage I, defined as boosting the energy of radioactive

<sup>\*</sup> Supplementary material in the form of a .pdf file available from the Journal web page at

<http://dx.doi.org/10.1140/epja/i2016-16334-4>

<sup>a</sup> e-mail: [mgb@cern.ch](mailto:mgb@cern.ch)

beams up to 5.5 MeV/u for  $A/q = 4.5$ . Section 3 gives more details on the different components of the project. The foreseen physics program is outlined in sect. 4 and some future prospects are given in sect. 5.

## 2 From idea to reality

ISOLDE celebrated the 50th anniversary of its approval in 2014 [3]. The capabilities of this ISOL facility have improved dramatically during the years, and its status has changed gradually, growing from an experiment into a facility fully integrated in the CERN infrastructure. The first incarnation of ISOLDE was placed at the SC accelerator and first radioactive beam was delivered in 1967. A major upgrade (ISOLDE 2) led in 1974 to a large intensity increase and a very productive period, which finally triggered the construction of a second separator with high resolution (ISOLDE 3) in 1987. When the SC accelerator was closed at the end of 1990 ISOLDE was integrated in the CERN accelerator complex through a move to the PS Booster where it is still situated and gradually has transformed into the current facility. We refer to [4–6] for a detailed overview of the evolution of ISOLDE and to [7] for a recent status report. A key ingredient to the long lifetime of the facility is the wide range of isotopes that can be produced by CERN high-energy high-intensity proton beams and the accumulated experience in construction of target-ion source units that provide purified beams of individual isotopes.

The proposal to reaccelerate ISOLDE beams to several MeV/u was put forward in 1994 [8] and was approved as experiment IS347. The first such reaccelerated beam had been delivered only a few years earlier in Louvain-la-Neuve, see [9] for a review of the first two decades of reaccelerated radioactive beams including that of REX-ISOLDE [10]. A special feature of REX-ISOLDE compared to other similar installations—but typical for the large installations at ISOLDE—is that it started up as an experiment being mainly funded from sources outside CERN. The current layout of the facility is shown in fig. 1.

A conceptual novelty of the REX-ISOLDE acceleration scheme was the decoupling of the production of radioactive ions from the single ionised to highly charged ions, the latter needed for efficient acceleration. The two steps can be optimised independently, and one can in particular benefit from the availability of many low-energy radioactive beams from ISOLDE. The low-energy beam is bunched in a Penning trap, ionised in an electron beam ion source (EBIS), mass separated, and accelerated in a linac, which for REX-ISOLDE is a conventional room temperature machine with several output energies initially between 0.8 MeV/u and 2.2 MeV/u [11]. All major components were funded by the REX-ISOLDE Collaboration, CERN contributed with an extension of the ISOLDE experimental hall that took place in the nineties.

REX-ISOLDE delivered its first radioactive beam in October 2001. Although it was originally motivated [8] by Coulomb excitation and neutron transfer on light ions

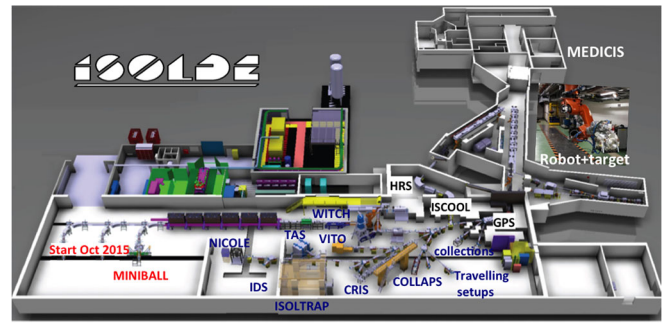


**Fig. 1.** Layout of the enlarged ISOLDE facility. The different parts of the facility and experiments are indicated: the two target stations are connected to the mass separators of low resolution, GPS and higher resolution, HRS. The location of the low-energy experiments COLLAPS, CRIS, IDS, ISOLTRAP, NICOLE, TAS, VITO and WITCH are indicated. The superconducting accelerator coupled to REX with the 6 cryomodules is shown. The ancillary buildings finished in 2012 to host the helium compressor station and the refrigerator cold box for the HIE-linac are shown. The site for the new CERN-MEDICIS facility starting in 2017 is also illustrated. The new robots in operation since 2014 are shown.

( $A < 52$ ), a much richer physics program was envisaged from the start. Already during the first year of running, proposals to upgrade the energy were put forward. A first step to 3.1 MeV/u could be accommodated in the existing buildings and was initiated immediately, but further steps (4.3 MeV/u and 5.5 MeV/u) were considered. They needed more space for the accelerator, motivating a further extension of the ISOLDE hall.

The science output from REX-ISOLDE has indeed gone much beyond the initial motivation, in particular after the upgrade to 3.1 MeV/u that was completed in 2004. The decoupling of the production and acceleration has allowed isotopes of many elements to be used in physics experiments (already 20 different elements were post-accelerated in 2008 [12]), for a selection of the many physics results see [10]. To give just one example, REX-ISOLDE has succeeded in accelerating very heavy nuclei such as  $^{220}\text{Rn}$  and  $^{224}\text{Ra}$  for measurements of their electric octupole moments [13].

The second extension of the ISOLDE experimental hall provided by CERN took place in 2004–5 and the experiments employing accelerated beams were moved into the hall late 2006/early 2007. However, the German funds that had provided for the linac up to 3.1 MeV/u could not be extended and a new framework was needed to ensure the continuation. Furthermore, superconducting technologies were being implemented in linear accelerators at TRIUMF and at Legnaro and seemed promising also for use at ISOLDE. To investigate the optimal scenario for the energy upgrade and to coordinate all other upgrade activities a steering group was set up at ISOLDE and the HIE-ISOLDE project launched [14]. An agreement to provide funding for the upgrade was made in 2004 by ISOLDE, Belgium, Denmark, Finland, Germany, Sweden and UK.

While the partners outside CERN started securing funding, the internal evaluation at CERN commenced with a scientific evaluation of its nuclear physics and astrophysics programmes including their future plans. The NuPAC workshop [15] in October 2005 led to a strong recommendation for the core of the HIE-ISOLDE plans, and work towards a project therefore started. As part of the project proposal preparation, an international advisory board recommended in 2006 to use the superconducting technology for the upgrade of the linac due to its higher flexibility, and R&D on this solution started soon afterwards. However, CERN was at this moment finishing the construction of the LHC and new projects could only be supported with substantial external contribution. As the preparations continued two reports collected the technical [16] and scientific [17] basis for the project. In May 2009 a new CERN management organised a special workshop on *New Opportunities in the Physics Landscape at CERN* [18] that also included a review of ISOLDE and its future. This led to the final approval of the HIE-ISOLDE project in 2009 by the Research Board and inclusion in 2010 of parts of its cost in the CERN budget.

A major part of the external contribution to HIE-ISOLDE has been covered by the ISOLDE Collaboration as well as by the EU-funded Marie-Curie initial training network within the FP7 program CATHI (Cryogenics, Accelerators and Targets for HIE-ISOLDE), but there have also been substantial contributions from Belgium and Sweden as well as other members of the ISOLDE Collaboration. The external contributions were essential for the initial R&D on the linac and for a large part of the beam quality improvement program. They provided full funding for the high-capacity ion-beam cooler ISCOOL that could be commissioned in the autumn of 2007 and for the substantial upgrade and renovation of the laser ion source RILIS taking place 2007–2011 [19,20].

### 3 The ISOLDE post-accelerator

#### 3.1 REX-accelerator elements

The REX-ISOLDE post-accelerator [21] provides RIB at energies ranging from 0.3 to 3 MeV/u for  $A/q \leq 4.5$ . The ISOLDE beams are charge bred with a combination of Penning trap and electron beam ion source providing low-emittance highly charged ion beams that can be post-accelerated in a compact normal conducting linac operating at a base frequency of 101.28 MHz, see fig. 2. Charge breeding is a key element of the concept of post-acceleration of RIB at REX-ISOLDE. ISOLDE delivers a quasi-continuous beam with a time structure dictated by the half-life of the nucleus of interest and its effusion and diffusion times in the primary target. The low-energy beam typically consists of singly charged ions of an energy between 30–60 keV. The transversal emittance of the ISOLDE beam is approximately three times larger than that of the charge breeder. To avoid transmission losses ISOLDE developed a unique system consisting in a Penning trap for accumulation, bunching and cooling

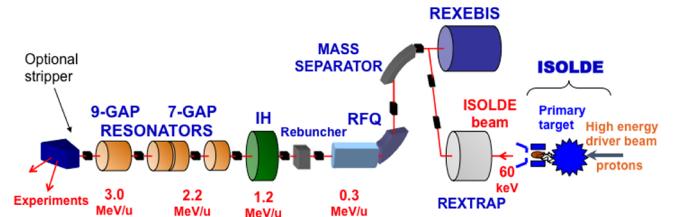


**Fig. 2.** REX layout: the singly charged ions from ISOLDE are captured and bunched in a large-acceptance Penning trap (REXTRAP) and charge bred in the REXEBIS ion source to an  $A/q$  ratio between 2 and 4.5. The ions are injected into a compact linear accelerator via a mass separator. The normal conducting linear accelerator consists of a Radio Frequency Quadrupole (RFQ), a rebuncher section, an Interdigital H-type (IH) structure, three seven-gap spiral resonators and a 9-gap IH resonator. The accelerator energy steps are shown and detailed in the text.

of the ion beam, REXTRAP, prior to an electron beam ion source (EBIS) for charge-state breeding in order to optimise transmission and functionality.

The design and construction of the REXTRAP was done at Mainz University and it is based on the design and experience of the ISOLTRAP mass spectrometer. REXTRAP [22] is a large cylindrical gas-filled Penning trap surrounded by a 3 T superconducting solenoid. The ions are electrostatically decelerated when they pass the potential barrier of the trap. At a certain gas pressure the ions that loose energy in the collision will not be able to leave the trap. The overall effect is a longitudinal cooling of the beam. After accumulation and additional radial cooling the barrier of the trap is lowered and the ions are released in a short pulse. To fulfil the transverse emittance condition of the REXEBIS transversal cooling is needed. This is achieved using the so-called side-band cooling method developed at ISOLDE [23]. The main advantage of the REXTRAP is that ions can be cooled very quickly. In fact the heavier the beam the faster the cooling. The buffer gas is typically Ne or Ar. The cooling time for  $10^{-4}$  mbar pressure of Ne is of the order of a few milliseconds. As this trap is designed to study rare exotic species the trapping volume is limited in size as is the number of stored and cooled ions. The REXTRAP efficiency is of the order of 50–60%. The energy spread of the beam depends on the size of the ion cloud and it can be up to 10 eV. A differential pumping system achieves good separation between the buffer gas-filled trap and the EBIS that operates at ultra high vacuum.

The REXEBIS is located in a platform above REXTRAP due to space restrictions. The beam transport system between the REXTRAP and the EBIS is designed to be achromatic and inject the pulsed beam with minimum losses. The transport line consists of two  $90^\circ$  bends and an intermediate straight section. The electron beam ion source achieves charge multiplication by electron bombardment. An electron gun at one end of the device produces an electron beam that is confined in a cylindrical volume over a distance of one meter by a magnetic

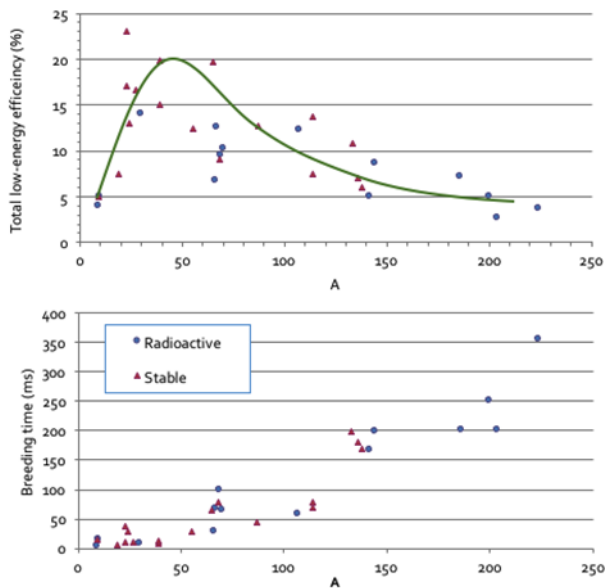


**Fig. 3.** Upper panel: total low-energy efficiency of REXTRAP and REXEBIS for some of the beams measured at ISOLDE. The continuous line is for visualization. Lower panel: the typical breeding times in REXEBIS. Courtesy of D. Voulot and F. Wenander.

solenoidal field with the axis of the field parallel to the direction of propagation of the electron beam. The REXEBIS potential is switched between ion injection and extraction. The quality factor of an EBIS is the electron beam density or the breeding time. The operational current density is around  $120 \text{ A/cm}^2$ , translating to a breeding time of 140 ms for  $^{140}\text{Ba}$  for example. The design and construction of the REXEBIS was done in Sweden at the Manne-Siegbahn Laboratory in Stockholm in collaboration with Chalmers University of Technology in Gothenburg.

The REXEBIS efficiency varies from a few percent to forty percent. Reference [24] gives more details on its performance. The efficiency, ratio of ejected ions to injected ones for a certain charge state, depends strongly on the injected current increasing for lower current. This partially compensates the decrease in yield when going to exotic species. The combined REXTRAP and REXEBIS efficiency measured for a selection of beams is shown in the upper panel of fig. 3. The breeding time in the EBIS depends of the  $A/q$  requested and the mass, reaching up to a few hundreds of milliseconds for the heavier species as shown in the bottom panel of fig. 3. The pulse extracted by the REXEBIS is a few tens of microsecond long. The pulse length can be extended from a few tens of  $\mu\text{s}$  to several hundreds of  $\mu\text{s}$  as discussed in [12]. Studies to go beyond this pulse length to a few milliseconds are already on going. The extraction potential is adjusted to give the correct injection energy for the Radio Frequency Quadrupole (RFQ).

One should note that it is necessary to mass separate the beam after the REXEBIS due to the presence of residual gas, mainly C, N, O, Ne and Ar. As the energy spread of the ion beam from EBIS is  $\Delta E/E \approx 5 \times 10^{-3}$  a Nier-type spectrometer was needed [25].

The REX-linac [26] consists of a low-energy Radio Frequency Quadrupole (RFQ) accelerator [27], a 20-gap interdigital H-type (IH) structure [28], and three 7-gap resonators [29] with a resonance frequency of 101.28 MHz. The energy acceleration of these three structures allow to increase the energy from the injection in the RFQ of 5 keV/u to 0.3 MeV/u and to 1.1–1.2 MeV/u in the IH structure.

The beam dynamics concept of the 20-gap IH structure requires a convergent beam in the transverse and longitudinal directions with small phase spread. Thus a split-ring rebuncher [30] is located between the RFQ and the IH. The IH accelerator design was based in the experience gained from the development of IH structures for GSI HLI [31] and CERN LINAC3 [32]. The resonator accelerates heavy ions with a maximum of  $A/q$  of 4.5 from 0.3 MeV/u to a final energy which can be continuously varied from 1.1 to 1.2 MeV/u. This feature of continuous final energy was a novelty with respect to its progenitors in the GSI or CERN linacs. The emittance growth in the IH structure is small, up to 10%.

The high-energy section of the REX-ISOLDE linac consists of three 7-gap resonators similar to those developed for the High Current Injector at the Max Planck Institute for Nuclear Physics in Heidelberg [33]. It was introduced to provide variable ion beam energies. It accelerates the ion beam from 1.2 MeV/u to final energies of 1.55, 1.88 and 2.2 MeV/u. The energy can be varied continuously from the injection value by increasing the voltage and switching on the next resonator. The beam spot after the 7-gap resonator is less than 10 mm.

In order to extend the nuclear reaction studies to heavier masses an upgrade to 3 MeV/u was proposed immediately after the successful start and realised soon after in 2004. The simplest solution was to include a 9-gap IH structure operating at 202.56 MHz. This structure was constructed at Munich as a modification of the 7-gap IH structure developed for the Munich Accelerator for Fission Fragments, MAFF [34].

The duty cycle of the machine is determined by the width of the REXEBIS pulse close to 1 ms and its repetition rate of 10 Hz for heavy ions, and up to 50 Hz for light ions. The largest mass-to-charge ratio of the ions is 4.5 limited by the IH structure. The measured energy accuracy of the IH structure and 7-gap resonators is 1%. The first RF amplifier of 9-gap resonators was limited in power reducing the duty cycle of the 9-gap for the maximum  $A/q$ . An upgrade of the 9-gap RF amplifier has been implemented in 2016 to remove the previous limitation. The high power should be controlled to avoid problems with the vacuum seals. The transmission of the linac is as good as 90%.

### 3.2 A boost for ISOLDE beams: HIE-ISOLDE superconducting linac

The HIE-ISOLDE project intends to upgrade the ISOLDE capabilities over a wide front. The impact of the increase of energy and intensity of the injectors together with improvements in several aspects of the secondary beam

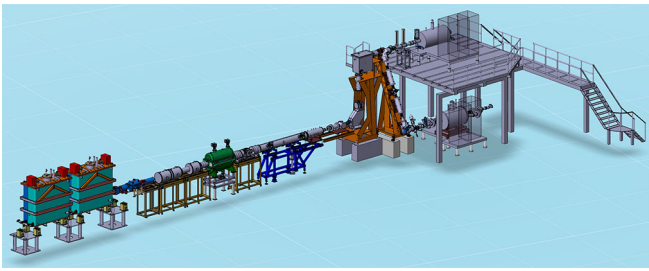


**Fig. 4.** 3D view of the post-accelerator at ISOLDE as it looks in 2016. It combines the exiting REX-linac with two superconducting cryomodules with a total of 10 quarter wave resonators cavities to boost the energy to 5.5 MeV/u for  $A/q = 4.5$ .

properties such as purity, ionisation efficiency and optical quality are addressed in the HIE-ISOLDE Design Study [35] that will be briefly discussed in sect. 3.3. Its implementation will be done gradually along the next decade. The reach of new physics comes from the increase of energy of the post-accelerated beam. The plan is to boost the maximum energy of the beams, going in stages from the previous energy of 3 MeV via 5.5 MeV to finally 10 MeV per nucleon for RIB, of  $A/q$  up to 4.5, by first extending and later replacing the 7-gap and 9-gap with superconducting cavities. The aim is to achieve full energy variability and operational flexibility while maintaining beam quality and keeping a very compact linac design compatible with the existing ISOLDE building.

The major component is the addition of a new superconducting (SC) linear accelerator (HIE-linac) based on quarter wave resonators. The HIE-linac upgrade is staged to deliver higher beam energies to the experiments as soon as possible. The first stage involves the design, construction, installation and commissioning of the first two cryomodules downstream of REX. Each cryomodule houses five high- $\beta$  ( $\beta_g = 10.3\%$ ) SC cavities and one SC solenoid. The geometrical  $\beta$ ,  $\beta_g$ , of 10.3% of the speed of light corresponds to the designed speed value of the beam for which the accelerating efficiency of the cavity is maximum. The first cryomodule was ready at the beginning of 2015 and the first radioactive beams were accelerated up to 4 MeV/u in the autumn of 2015. Two cryomodules are already at the ISOLDE hall while writing these lines in the spring of 2016. Figure 4 shows a 3D drawing of the HIE-ISOLDE stage I linac where the first two cryomodules are coupled to the previously existing REX-linac. One extra cryomodule will be added in 2017 prior to the experimental campaign and the fourth one, completing stage II, at the beginning of 2018 in order to reach the expected 10 MeV/u for  $A/q = 4$  as shown in fig. 5. For more details see [36–38].

In a third stage it is planned to substitute the 7-gap resonator and 9-gap structure of REX with two cryomodules housing six low- $\beta$  ( $\beta_g = 6.3\%$ ) SC cavities and two SC solenoids. The advantage of the use of superconducting cavities is the capacity of decelerating the beam. This capacity will open a new range of energies not previously accessible with REX due to the fixed velocity profile of the 20-gap IH-structure. The tunable low accelerating en-

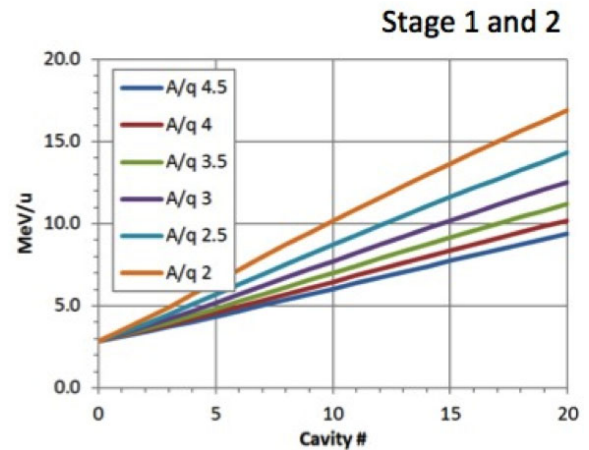


**Fig. 5.** The output energy for the beam is given *versus* the number of cavities for different values of  $A/q$  from 2 to 4.5.

ergies open many possibilities for reaction studies of astrophysical interest and for solid-state physics. It is also foreseen to insert a pre-buncher to the RFQ accelerator at a sub-harmonic frequency allowing the bunch spacing to be increased without significant loss in transmission. The addition of a beam chopper between the RFQ and the IH has been considered to clean the background of satellite bunches. The timeline for the third stage is not yet defined.

Considering that the present technology allows an accelerating field per cavity of 6 MV/m, the beam dynamics studies [39, 40] confirmed that this field per cavity fulfil the requirements of limited space in the experimental hall and maximum dynamical acceptance and optical performance of the machine. This requirement influences the specification of the SC solenoid, the alignment and beam diagnostic systems, the steering magnets and the cryomodule. The final energies of the ion beam, depending on the number of cavities and  $A/q$ , are shown in fig. 5.

The high- $\beta$  cavities used at HIE-ISOLDE adopted a technology based on copper cavities sputter-coated with niobium. The technique was invented at CERN for the cavities of LEP [41] using magnetron sputtered Nb films on elliptical cavities. The HIE-ISOLDE cavity design is inspired by those developed at INFN-Legnaro to accelerate heavy ions at the ALPI-linac [42]. The HIE-ISOLDE cavities are machined from bulk Cu to reduce the number of electron beam weldings. The shape of the helium reservoir was modified to reduce sensitivity to helium pressure fluctuations. The work at CERN to establish the complete coating and production method for Nb sputtering cavities started in 2008. By the end of 2009 the chemistry, coating and RF infrastructures were operational. Much effort was put in the optimisation of the coating process, reaching in the prototypes 30% better performance than the design goal [43]. This optimum performance could not be reproduced in the series production of the cavities due to defects in the copper substrate produced in industry. Figure 6 shows the design of the cavities used as well as that of the power coupler.

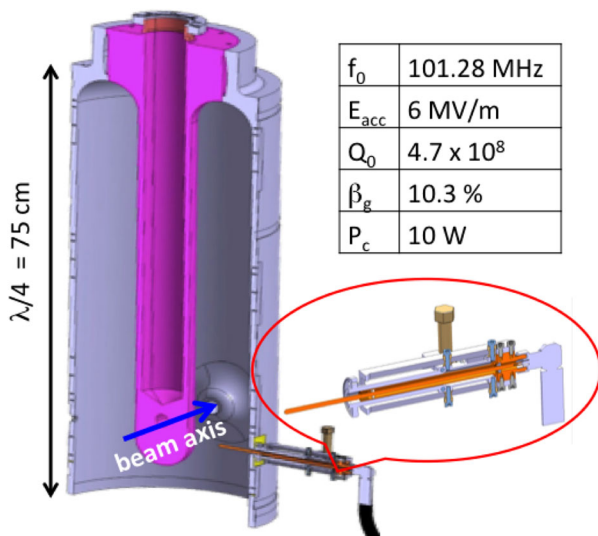


**Fig. 6.** On the left the 3D drawing of the QWR cavities with a length of 75 cm and a width of 30 cm. The ions are accelerated by the resonating field of the cavity. The power coupler on the right allows the field in the cavity to resonate. The table lists the main parameters of the cavities: frequency, maximum accelerating field, quality factor,  $\beta$  value and the expected heat dissipation.

The power coupler and tuning system of the cavities were designed at CERN. The coupler is based on a stainless-steel external body to minimise the thermal load on the cavity and a displacement system and guidance rails of stainless steel to ensure positioning of the antenna in the cryogenic environment. Experience has shown that the antenna has to be able to dissipate the heat much faster. The coupler has been revisited and a new design implemented including a new antenna made of copper and welded to the inner conductor of the connector. For more details on the mechanical design see fig. 6.

The low-level RF system excites and keeps the cavity field stable at the requested operating point. The accelerating voltage and phase can be changed in seconds to adapt the linac for a new ion species. Transverse beam focusing at the HIE-ISOLDE linac is provided by superconducting solenoids integrated in the common vacuum cryostat. The presence of neighbouring superconducting cavities imposes tight specifications on the remanent magnetisation to avoid flux trapping and on the stray field at nominal current.

A stainless-steel vacuum vessel houses the five cavities and the solenoid surrounded by a thermal screen which is actively cooled with helium at 50 K. In order to minimise the drift length between cavities and the overall length of the machine a common vacuum was chosen for the beam and cryogenic insulation. A photo of the inner elements of the cryomodule including the five cavities, the helium vessel on the top and the solenoid hidden behind the support frame is shown in fig. 7. To run the linac in optimum conditions the active components, cavities and solenoid, must be aligned within a precision of 0.3 mm on the REX beam line and possible changes monitored within a tenth



**Fig. 7.** The picture, taken in April 2015, shows the complete assembly of the first cryomodule. One can see the 5 cavities, the helium vessel on the top and the support frame hiding the solenoid placed between the third and fourth cavity.

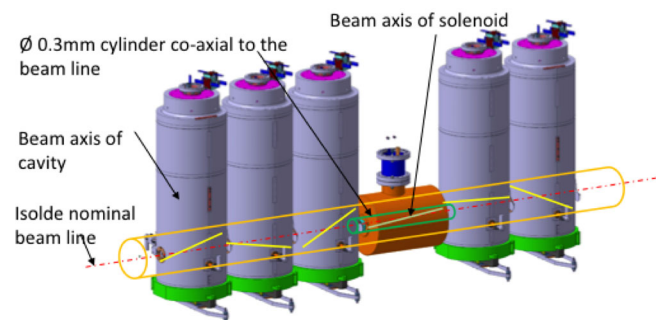


**Fig. 8.** 3D drawing of the internal elements of the cryomodule. The alignment specifications require that every cavity beam port must be contained in a cylinder of 0.6 mm and 0.3 mm for the solenoid centred in the beamline.

of a millimetre. The elements and tolerances for the alignment of the HIE-ISOLDE cryomodule are shown in fig. 8. The machine relies on the controls infrastructure already deployed in the CERN accelerator complex. The cryogenic system includes one cryogenic transfer line, which links the cold box and the different interconnecting boxes feeding from above all cryomodules of the HIE-linac.

Although the major challenge was to produce cavities achieving the required performance, the assembly of the cryomodule also presented great difficulties as all the elements are located in the same vacuum vessel. Materials have been specially chosen to ensure that the components can be properly cleaned and that the quality of the performance of the cavities is stable over time. After a delicate assembly phase, the first cryomodule was transported to the ISOLDE hall on May 2nd, 2015 and coupled to the existing REX-ISOLDE. Since April 2016 the first two cryomodules completing stage I of the HIE-ISOLDE project



**Fig. 9.** The ISOLDE post-accelerator with two cryomodules is shown in the photo taken inside the linac tunnel. Radioactive beams up to 5.5 MeV/u are expected for the end of August 2016.

are in the ISOLDE hall cooled and ready to start the commissioning, see fig. 9.

The full accelerating voltage of a superconducting linac is available for all  $A/q$  as the phases can be independently adjusted for each cavity. This implies that the maximum energy (in MeV/u) is dependent on the  $A/q$  value. The design energy of HIE-ISOLDE with 4 cryomodules is 10 MeV/u for  $A/q = 4$ . The maximum energy will increase to 14.3 MeV/u for  $A/q = 2.5$ , see fig. 5.

### 3.2.1 High-energy beam transfer and experimental beam lines

A new high-energy beam transfer line, HEBT, brings the beam into the extension of the ISOLDE experimental hall built in 2006. The HEBT has been designed to preserve the beam emittances. This requires the minimisation of the drift space between accelerating cavities reducing the longitudinal distance in the interconnection regions. The space between two cryomodules is only 370 mm of which 90 mm are available for specially designed very short diagnostic boxes. The HEBT transport system can manage beams with rigidities up to 2 Tm and is based on a periodic doublet lattice with a period length of 2.62 m equal to the period length of a single high- $\beta$  cryomodule. The choice of the period length minimises the disruption of the transfer line every time a new cryomodule is added to the accelerator.

The drift sections outside the accelerator tunnel include two dipole magnets to produce a 90° bend to steer the beam to the different experimental stations. Three identical beamlines are planned, two of them are already operative since 2015 and the third one will be mounted in the winter of 2017 together with the third cryomodule. Further steering magnets will be fitted in this confined space in order to correct the trajectory of the particles. Horizontal and vertical corrector magnets are installed adjacent to every diagnostic box, see fig. 10.

New beam diagnostic elements have been developed for HIE-ISOLDE to provide measurements of intensity, energy and transverse profiles. The magnetic fields of the

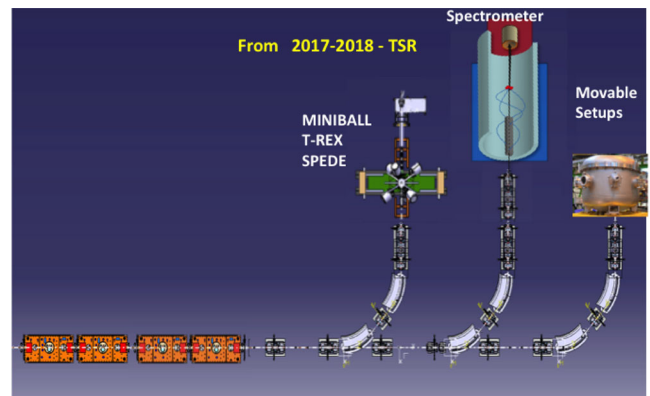


**Fig. 10.** The post-accelerator and beamlines as expected in 2017-2018. The four cryomodules will be mounted and the three beamlines operative with the planned instrumentation.

HEBT will scale with the beam energy. The measurement of the beam current is essential in order to determine and optimise the transmission. The stable beam will have currents in the order of 1–100 pA while radioactive beams can be as low as a few ions/s. The HEBT design is made to achieve an absolute transport efficiency close to 100%.

All required beam diagnostic instruments are integrated in octagonal-shaped vacuum chambers with five radially distributed ports available for the installation of instruments or collimating devices plus a port for vacuum pumping. All diagnostic boxes have Faraday cups, collimators of different diameters and V-shaped slits. Both collimators and slits are mounted on a blade. All elements are movable using a stepping motor. Depending on the Faraday cup size, one has short and long diagnostic boxes. The former are placed between cryomodules, the latter before the first cryomodule and in the beamlines after the SC linac. The diagnostic boxes before and after the dipoles are furnished with variable large slots with the purpose of limiting and even measuring the energy spread, for that they are equipped with a commercial passivated implanted planar Si (PIPS) detector. Carbon stripping foils with different thicknesses are used for beam purification. The foils are presently installed in the diagnostic boxes before each dipole in the second beamline, XT02. Installation of the stripper foils in equivalent positions are foreseen for the other beamlines. The placement of Si-telescope in the last diagnostic box before each of the experimental device is planned to determine the composition of the post-accelerated beam.

Intensity values down to 0.1 nA are measured with the Faraday cups. The beam transverse profile is measured by V-shaped slits moved in front of the Faraday cup. that here can achieve a resolution of tenths of mm. The diameter of the Faraday cup is 30 mm so the slits are able to scan the beam width and height. The position of the beam is determined with an accuracy of 0.2–0.3 mm for stable beams. The beam energy has to be measured from 0.3 MeV/u to 10 MeV/u. Beam energy and longitudinal profiles are determined by the use of Si detectors. As explained in sect. 3.2.2 the most precise measurement of the

radioactive beams will be obtained using the time of flight between different Si detectors.

A layout of the HEBT and the already commissioned beamlines is shown in fig. 10. In the first beamline, XT01, the MINIBALL detector is assembled with the CD and alternative use of T-REX and SPEDE are foreseen, for more details of these devices see sect. 3.4 dedicated to instrumentation. In the second beamline, XT02, general purpose scattering chamber is installed to do reaction studies, other movable devices are also planned for this beamline. The future layout will include the fully functioning three beamlines incorporating the ISOL solenoidal spectrometer, ISS, for transfer reaction studies in XT02. The scattering chamber mentioned above and other travelling experiments will be allocated to the third beamline, XT03 as shown pictorially in fig. 10.

### 3.2.2 Beam commissioning and operation of REX/HIE-ISOLDE

The beam commissioning of the post-accelerator started in June 2015 after the refurbishment of the REX normal conducting linac was completed.

Different pilot beams produced in the EBIS with different  $A/q$  were used to phase the cavities. The beam commissioning was done in different steps. The beam coming from the RFQ was used to re-commission the REX diagnostic box. Then it was transported to the first HIE-ISOLDE diagnostics box and used to commission the Faraday cup, the silicon detector and the scanning slits. Further the beam from REX was drifted through the cryomodule while the superconducting cavities were off. This beam was used to commission the diagnostics and the optical elements of the linac and the first beamline, XT01. Afterwards the silicon detector was used to determine the needed RF power out of the amplifiers and to phase each of the accelerating structures. Finally the beam was transported along XT02 and the different elements of the line were tested.

Operations started in mid-October 2015 using first the stable  $^{87}\text{Rb}^{28+}$  beam from the target coupled to the general purpose separator (GPS Target) and it was accelerated up to 2.85 MeV/u in the REX normal conducting linac. In addition, stable  $^{12}\text{C}^{4+}$  produced in the EBIS, was used as a pilot beam to phase the superconducting cavities and to set up the beamlines as described previously. On October 19th, the first experiment of the campaign started with the delivery of stable  $^{22}\text{Ne}^{7+}$  with an energy of 2.85 MeV/u to the MINIBALL experimental station. The first 4 MeV/u radioactive beam was delivered a few days later on October 22nd. The 4 MeV/u beam time was limited to 6–8 hours per day due to an overheating problem in the couplers of the superconducting cavities. A beam with the REX-linac final energy was used for the remaining hours of the day. Over the following weeks, different charge states of two zinc isotopes  $^{74}\text{Zn}$  and  $^{76}\text{Zn}$  with energies of 2.85 and 4 MeV/u were sent to the experimental station.

Characterising the energy of the beam accurately and precisely as well as its stability is critical for most of the experiments. Three different instruments were used to measure the beam energy during 2015: silicon detectors, the RF calibration of the accelerating structures and the first dipole of the HEBT line. The three measurements produced results consistent within 2–3%. Silicon detectors implemented in the diagnostic boxes were used throughout the physics campaign and proved to be the most versatile of all the three detector systems. However, measurements in their current configuration are time consuming. The counting rate of the detector is limited by the repetition rate of the linac since a few hundred microseconds in between events are needed for the detector to distinguish them apart. Since the repetition rate of the machine in 2015 was limited to 10 Hz, a typical measurement took  $\approx 15$  mins. Absolute energy calibration of the detectors is difficult, for more details, see [44]. Additionally in 2016 silicon detectors (a ring-shaped one and disk-shaped one) separated by 7.8 meters will be used to measure the Time of Flight (TOF) of the ions [45]. This method should allow to achieve an uncertainty of 0.5 ns. This translates for a beam of 5 MeV/u into a 0.4% uncertainty in the total energy of the beam.

Residual gas in the REXEBIS will unavoidably be ionised and transported to the REX separator together with the beam of interest. These contaminants will be transported to the linac if their  $A/q$  are identical or very close to that of the RIB of interest. Any other impurities coming from the target with the same mass number, close atomic number and long enough half-lives may also reach to the experimental station. The silicon detectors cannot be used to distinguish these contaminants since they have very similar total energy. Therefore a Si-telescope will be implemented in the movable arm of the last diagnostic box before the experimental devices.

The post-accelerated beam will have a 9.87 ns (*i.e.*, 1/101.28 MHz) time microstructure produced by the bunching in the first few cells of the RFQ. This is within a macrostructure produced by the necessary charge breeding time. With the upgrade of the 9-gap RF amplifier installed in 2016 the post-accelerator will be able to deliver beams with  $A/q$  up to 4.5, maximum repetition rate 50 Hz and the longest pulse length 2 ms. However, it should be noted that it will not be possible to push the three parameters to the limit at the same time.

### 3.3 Intensity, purity and beam quality upgrades

In the period since 2010 much progress has also been achieved in the design study to further improve the beam intensity and quality. Progress done on different fronts will be described.

Beam intensities can be increased by research in new target materials and by improvement of the efficiency of the targets and ion source systems. This has been the way pursued by the ISOLDE technical team along the years. An alternative way and sort of “brute force” method for increasing the beam intensity is to raise the intensity of the

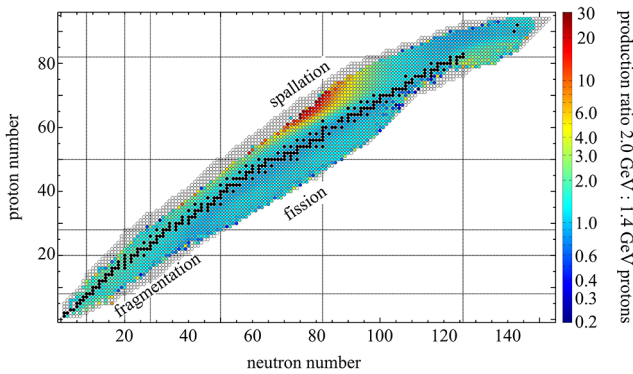


**Fig. 11.** The expected ratio across the nuclear chart for 2 GeV versus 1.4 GeV protons on a 62 g/cm<sup>2</sup> thick uranium target. The regions where the fragmentation, fission and spallation processes dominate are indicated. Courtesy of A. Gottberg.

primary proton beam to ISOLDE. There has been much activity on high-intensity high-energy proton accelerators during the last decades since they are required for many projects: intense neutron sources such as the ESS [46], driver accelerator for neutrino physics, transmutation of nuclear waste, and EURISOL [47], the ambitious plans for a future high-intensity ISOL facility.

CERN has been active in this field in order to upgrade the existing injector accelerator chain. The very first step in the chain, a proton linac, will be replaced by the newly built LINAC4 in 2019 [48,49]. This will allow the proton beam intensity for ISOLDE to increase by a factor of 3. This increase of intensity by the proton injector requires an upgrade of the different accelerators at CERN to assure an increase of brilliance of the Large Hadron Collider, LHC. As a result of this study it was found and presented in the 2010 Chamonix workshop that an increase of beam energy of the Proton Synchrotron Booster, PSB, from 1.4 GeV to 2 GeV will ease the injection of high-intensity and brilliance beam in the Proton Synchrotron [50]. The energy upgrade of the PSB [51,52] is planned for the second CERN long shutdown, 2019-2020.

The production yield (number of ions/s or ions/ $\mu\text{C}$ ) of a certain nucleus ( $Z, N$ ) is proportional to the target thickness, proton beam intensity, production cross-section and several efficiency factors such as release time, ionisation potential, mass separation and transport. The production cross-section depends on the energy of the incoming beam and the cross-section of the dominant nuclear reaction. Three main nuclear reaction channels can be triggered upon interaction of the high-energy high-intensity protons from the CERN injector PSB with the target nuclei: spallation, fission and fragmentation. Simulations have been done using the ABRABLA code [53] for direct reactions and FLUKA [54] for inclusion of secondary process relevant in thick targets. It is found that an increase of a factor of two to five is expected for the fragmentation process, up to a factor of ten for the spallation process and similar production for fission products. The expected increase in production for 2 GeV compared with 1.4 GeV protons for a UC<sub>x</sub> target is shown in fig. 11. In the former case

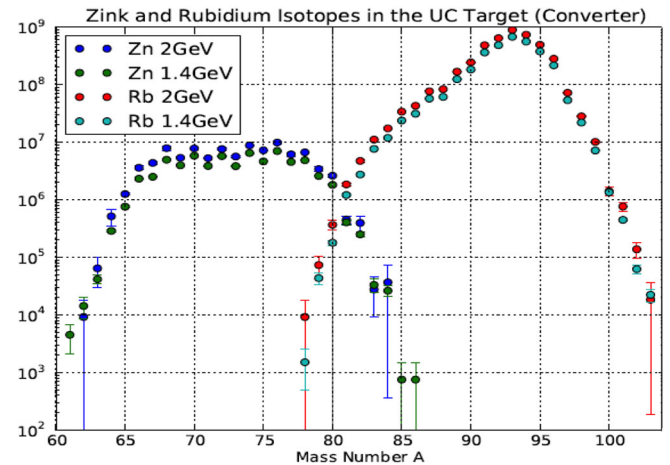


**Fig. 12.** Comparison of the expected production for the fission products Zn and Rb from a UC<sub>x</sub> target with a neutron converter for proton bombarding energies of 2 GeV and 1.4 GeV. An increase of a factor of 1.4 is expected.

**Table 1.** Expected power increase on ISOLDE targets due to the increase of energy and intensity of the incoming proton beam from the PS-Booster injector. Values taken from [55].

Protons /pulse	Intensity ( $\mu\text{A}$ )	Energy (GeV)	cycle (s) (s)	Power (kW)
$3.3 \times 10^{13}$	2.2	1.4	1.2	3.1
$1 \times 10^{14}$	6.7	1.4	1.2	9.3
$1 \times 10^{14}$	6.7	2.0	1.2	13.3

the use of a neutron-converter can give an increase of up to a factor of 1.4, see fig. 12. Based on these encouraging results a proposal to extend the 2 GeV proton energy to ISOLDE was presented to the ISOLDE Neutron Time-of-Flight Committee, INTC, in November 2012. The integration study required by the CERN research board was done in the spring of 2015. It was concluded that the implementation will be done most likely in the third long shutdown.

Table 1 shows the expected increase in intensity and power considered in the HIE-ISOLDE Design study and published in [35,55]. At the beginning the proton/pulse intensity for ISOLDE will be limited due to aperture restrictions in the PSB ejection line to 4.3  $\mu\text{A}$ . This corresponds to 2 GeV energy of the proton pulse to an average power on target of 8.6 KW.

Such upgrades will have immediate effect on the ISOLDE target area. A considerable effort has gone into studying the impact on the operation and maintenance of the facility. Issues such as resistance of the target materials, target overheating, target lifetime as well as effects on the target stations, the beam-dumps, shielding, ..., etc. have been addressed in the HIE-ISOLDE design study [55]. As a conclusion it was found that some elements require modifications to accommodate an increase in energy and/or intensity of the proton beam on target. The expected yields across the nuclear chart for 2 GeV

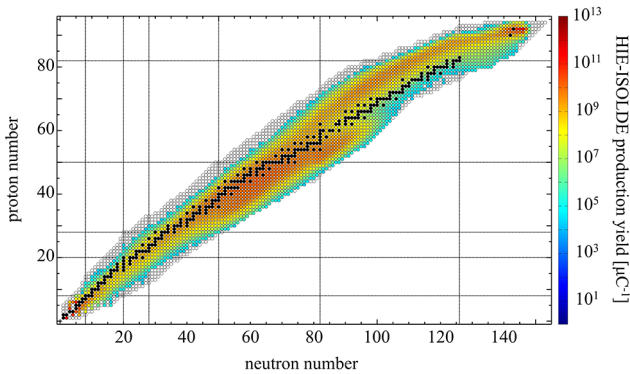


**Fig. 13.** The FLUKA [54] expected yields in  $\mu\text{C}^{-1}$  across the nuclear chart assuming HIE-ISOLDE conditions, *i.e.* an energy of 2.0 GeV on a  $62\text{ g/cm}^2$   $\text{UC}_x$  target thickness in a cylinder of 1.8 cm diameter and 18 cm length surrounded by the conventional ISOLDE graphite sleeve and tantalum target container. Courtesy of A. Gottberg.

protons on a  $62\text{ g/cm}^2$  thick (corresponding to  $52\text{ g/cm}^2$  depleted uranium target)  $\text{UC}_x$  target in a cylinder of 1.8 cm diameter and 18 cm length surrounded by the conventional ISOLDE graphite sleeve and tantalum target container are shown in fig. 13. One of the key issues associated with a proton intensity and energy upgrade is the evaluation of the required shielding. Two actions have been done at ISOLDE in this respect: separate the ventilation of the target zone from that of the class A laboratory and improve the air tightness of the target area to reduce the current extraction rate of  $7200\text{ m}^3/\text{h}$  [55]. Furthermore the ISOLDE beam dumps were revised as they were designed for taking up to 1.5 kW proton power. The existing beam dumps are steel blocks with dimensions of  $1.6\text{ m} \times 1.6\text{ m} \times 2.4\text{ m}$  in the target coupled to the GPS and  $0.4\text{ m} \times 0.4\text{ m} \times 1\text{ m}$  in the one coupled to the high-resolution separator, HRS, surrounded by concrete shielding, see fig. 1. In addition investigations done during the CERN long shutdown showed that the GPS beam dump is largely misaligned with respect to the proton beam. Although the exact heat transfer coefficient around the dumps is not known, simulations using the ANSYS code indicate that the situation will be critical if the HIE-ISOLDE parameters are adopted. New beam dumps, possibly with forced water cooling should be installed at ISOLDE prior to any substantial increase in intensity or energy of the proton beam can be considered. The replacement of the beam dumps is not a trivial matter due to their location underground.

The bottleneck of any ISOL facility is the fact that the ionisation process depends on the chemical properties of the desired element. At the level of improvement of ionisation the largest boost has come with the arrival of the high-power lasers to promote the ionisation of a certain isotope. The Resonance Ionisation Laser Ion source (RILIS) is an efficient and selective way of ionising the reaction products to produce a beam of a chosen isotope. Several developments have been done recently such as the use of a remote controlled narrow line-width mode of op-

eration for the recently installed Ti:sapphire laser, production of isobar free ionisation using the laser Ion Source Trap (LIST), or isobar selective particle identification using the multi-reflection time-of-flight mass spectrometer (MR-ToF) [56,57]. The latter combination is so sensitive that it has allowed to observe surface ionised iron in sufficient amounts to allow for the validation of the ionisation scheme.

Building upon the ISOLDE Cooler and buncher experience, a redesigned high-resolution separator incorporating a new RFQ cooler has been studied. The design of a new Radio Frequency Quadrupole Cooler and Buncher (RFQCB) will address issues, gas pressure stability, vacuum pressure variation through the system and the ion optics to facilitate compatibility with other beamline components. A prototype design is currently under fabrication and it will be integrated in the layout of the off-line separator. The prototype will address the problem of space charge limit of  $10^8$  ion/s of the present device as well as ion beam transmission and bunch width as a function of the cooling time.

Improved mass resolution is a major goal of the beam quality upgrade. The existing high-resolution separator (HRS) can provide  $M/\Delta M$  between 3000 and 6000, much lower than the design value of 10.000 units. Studies have been done and two scenarios have been investigated: one with both a  $120^\circ$  and  $90^\circ$  dipole C-magnet and the other with two  $90^\circ$  magnets and a  $60^\circ$  pre-separator. The final decision will depend on the performance and position of the RFQCB, the optics of the beam and by the available space at the present facility. At present the one including the  $120^\circ$  dipole magnet is contemplated as the most favourable one. There are also plans to study the installation of a general purpose multi-reflection time-of-flight mass spectrometer based in the experience gained with the existing MR-ToF of ISOLTRAP [58].

As part of the HIE-ISOLDE design study an upgrade of the EBIS has also been addressed. A new EBIS has been designed with higher electron beam energy and density that will give faster charge breeding, preliminary tests are going on in collaboration with Brookhaven National Laboratory. The REXEBIS new design will focus on improvement of the repetition rate from the present 10 Hz to 100 Hz [59,60]. This will be achieved by addressing the ultra high vacuum, the electron current and density, the high voltage and the magnetic field. Presently a prototype of the electron gun exists and it has been tested at Brookhaven.

### 3.4 Instrumentation

The physics instrumentation that existed at REX-ISOLDE will continue to be available at HIE-ISOLDE and more instruments will be added to take full advantage of the increased experimental possibilities.

For much of the currently planned experimental programme the high-resolution gamma-ray detector array MINIBALL [61] is a key instrument, see fig. 14. It consists of 24 six-fold segmented high-purity germanium crys-

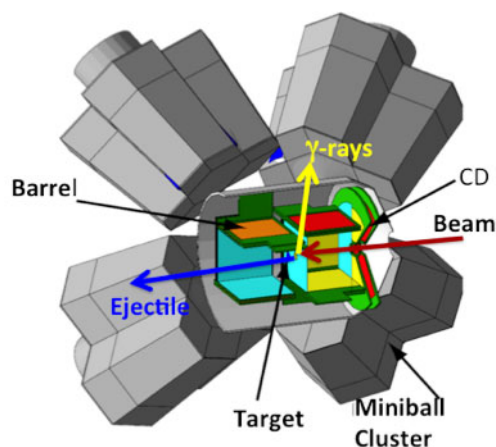


**Fig. 14.** The MINIBALL high-resolution gamma-ray detector array is shown here in the configuration surrounding the T-REX Si strip detector array. The beam is entering from the right through a CD detector and react in the target situated in the middle of the barrel detectors.

tals which in close configuration, as employed for Coulomb excitation experiments, cover about 60% of the full solid angle and give a photo-peak efficiency at 1.3 MeV of about 8%. The design of the array was made with a focus on efficiency rather than multiplicity capability, since the typical gamma-ray multiplicities in radioactive-beam experiments is low compared to what is met in high-spin experiments. There is still a need for high granularity, so that Doppler corrections can be made. This is achieved partially through the segmentation, which has in practice given sufficient accuracy with the beam obtainable at REX-ISOLDE. Pulse-shape analysis will allow to improve the granularity even further. Two target chambers have been used so far. The first and smallest is used for Coulomb excitation and contains apart from the target a Double-Sided Si Strip Detector (DSSSD) of CD design for detection of the outgoing charged fragments. Further downstream a Parallel-Plate Avalanche Counter (PPAC) or a Bragg ionisation chamber can be placed. Active collimation with Si PIN diodes or diamond detectors have also been used. The second and larger target chamber contains the T-REX [62] Si detector array. As shown in fig. 14 it consists of eight barrel detectors immediately before and after the target plus two circular CD detectors at the entrance and exit of the chamber, all detectors subdivided in strips to give a high granularity. The total solid angle is about 66% of  $4\pi$ . This set-up is optimised for transfer experiments in inverse kinematics. The Ge detectors will in this configuration have an absolute photo-peak efficiency of about 5%.

There is a strong wish from a large part of the community to supplement MINIBALL with a zero-degree spectrometer to enable detection of heavy beam-like fragments. Among the possibilities the integration of part of the TRI $\mu$ P spectrometer [63] from KVI is the favourable choice. Simulations of the integration in the hall and of the beam optics has been started, but the final implementa-



**Fig. 15.** 3D drawing of the possible integration of a zero-degree spectrometer after the MINIBALL array for the identification of the ejectiles in transfer reactions of high energy.

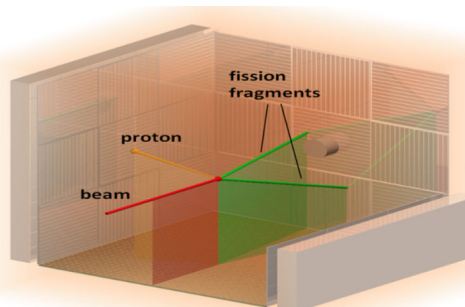


**Fig. 16.** Sketch of the active target principle. The beam goes through a gaseous target and will along with all charged reaction products cause ionization in the gas. The electrons drift in an electric field and are amplified and recorded, enabling the reconstruction of the tracks. Courtesy of G.F. Grinyer.

tion has not been decided. One scenario is shown in fig. 15. For the reaction studies, where gamma detection is of less importance, other set-ups may be more optimal. A large scattering chamber has already been constructed by the Lund group and used for proton elastic resonance scattering of a  $^{30}\text{Mg}$  beam [64] at REX. It is presently sitting at the second beamline, XT02.

In many situations, such as the elastic resonance scattering just mentioned, one may gain in sensitivity by having an active target [65]. This is very useful for low-intensity radioactive beams since one effectively has a thick target, but there are obvious limits to what detector materials can be used. Gaseous detectors may allow the reaction vertex to be determined with good position resolution and much of the technology can be taken over from high-energy experiments. A pioneer among detectors used at a few MeV per nucleon is MAYA [66] that has been employed already at several radioactive-beam laboratories. A second-generation detector, ACTAR [67] shown in fig. 16, is currently under development, but several other projects exist as reviewed in [65]. One of them is the optical time projection chamber (OTPC) that has so far mainly been used for decay studies [68]. It benefits from having a strongly reduced sensitivity to beta particles, only heavy emitted charged particles (among them nuclear recoils) leave a track. The decaying nuclei must

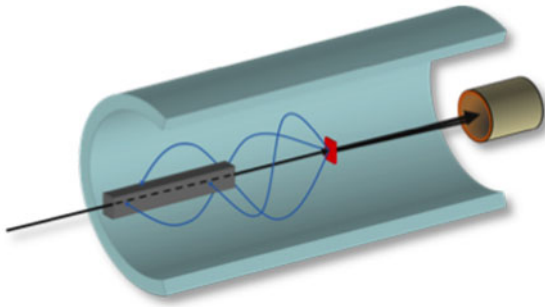


**Fig. 17.** The principle behind the ISOL Solenoidal Spectrometer, ISS, is illustrated. The beam enters from the left through a detector box and reacts in the target placed in the middle of the magnetic field. Charged reaction products are bent in the strong magnetic field (field lines parallel to the beam axis) and focused unto the detector array. The position, energy and time of flight of the particle allow to entangle the reaction kinematics.

be implanted into the detector and must therefore have beam energies of at least a few MeV per nucleon.

There are advanced plans to install the so-called ISOL Solenoidal Spectrometer, ISS, similar to HELIOS, existing at Argonne [69], fig. 17. It addresses the “kinematic compression” problem that transfer reactions such as (d,p) have at backward angles in inverse kinematics, namely that the excitation energy scale for a given angle is compressed relatively to the one in the centre-of-mass system. A large superconducting solenoid bends the (low-energy) light particles emitted at backward angles unto a Si detector array placed around the beam axis. Position, energy and time measurement gives sufficient information to extract particle type, outgoing angle as well as an improved energy determination. The confinement of charged particles in a large magnetic field will also be attractive for active targets. An interesting current development is the scintillator detector array SpecMAT [70] that will allow detection also of accompanying gamma rays.

Tilted-foils polarization has been implemented at REX-ISOLDE and can be taken over at HIE-ISOLDE. The results attained so far are a nuclear spin polarization of  $3.6 \pm 0.3\%$  as measured with a  $\beta$ -NMR set-up [71].

The SPEDE conversion electron spectrometer [72] will be combined with the MINIBALL array for combined electron and gamma-ray spectroscopy. It is currently being installed at HIE-ISOLDE. The experience from the SAGE spectrometer [73] installed at the RITU gas-filled recoil separator at JYFL is very encouraging, in particular for studies of heavy nuclei.

## 4 Physics programme

A facility upgrade of the magnitude of the HIE-ISOLDE project implies that the physics programme enables users to address most aspects of modern nuclear structure. This is also reflected in the overview [17] of the scientific opportunities generated by HIE-ISOLDE. Rather than repeating this general point, we choose here to illustrate it

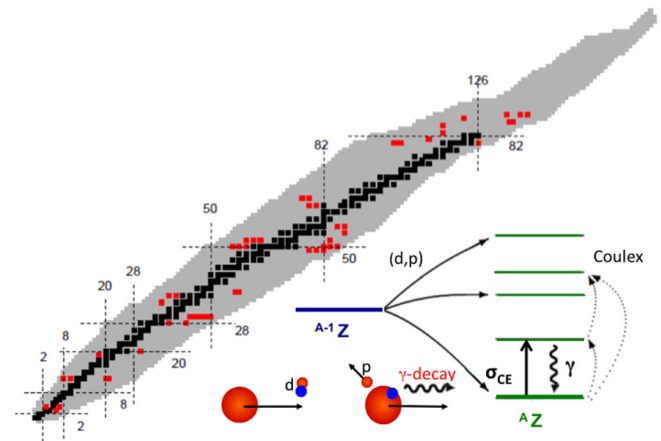


**Fig. 18.** Chart of the nuclides. Nuclei marked in red are the object of approved HIE-ISOLDE proposals. In the bottom part two commonly employed reaction types are sketched: Coulomb excitation (dotted lines) that favours collective excitations within a nucleus and transfer reactions (full lines, here one-neutron transfer) that favour single-particle transitions between neighbouring nuclei. The two reactions give complementary structure information.

by examples from the proposals already approved by the CERN scientific committees to run at the new facility. The emphasis will be on reaction experiments, but it should be noted that essentially all experiments at ISOLDE will benefit from the intensity increase and the improvements in beam purity and quality.

Figure 18 shows the approved beams for studies at HIE-ISOLDE up to February 2016 and table 2 lists all the proposals for experiments with accelerated radioactive beams at HIE-ISOLDE that have been accepted so far. A few of the letters of intents (LoIs) are included as well. Other ideas were put forward at the initial call for LoIs in the summer of 2010. The majority of the accepted proposals make use of Coulomb excitation of the beam, but there are also a substantial number of transfer reactions proposed. We shall refer to the experiment numbers as given in table 2 in the discussion below of individual proposals.

### 4.1 Nuclear reactions

There are some immediate experimental consequences of the increased beam energy at HIE-ISOLDE: the energy loss,  $dE/dx$ , of the beam in a target decreases slightly and the kinematics of the outgoing fragments change, *e.g.* increasing the Doppler shift of outgoing gamma rays. Much more important for the following discussion is that the reaction mechanisms evolve significantly from 3 MeV/u to above 5 MeV/u. The inelastic reactions are enhanced compared to elastic ones, there is a clearer separation between compound and direct type reactions, and there is more structure in the particle angular distributions that can contain higher angular momenta.

As illustrated schematically in the bottom part of fig. 18 different types of reaction address different nuclear

**Table 2.** Accepted proposals until February 2016 for accelerated radioactive-beam experiments at HIE-ISOLDE. The detailed proposals can be found via the website <http://isolde.web.cern.ch/active-experiments>.

Exp.	Title	Spokesperson(s)
IS546	Study of the effect of shell stabilization of the collective isovector valence-shell excitations along the $N = 80$ isotonic chain	C. Bauer, N. Pietralla, G. Rainovski
IS547	Coulomb excitation of the two proton-hole nucleus $^{206}\text{Hg}$	Z. Podolyák
IS548	Evolution of quadrupole and octupole collectivity north-east of $^{132}\text{Sn}$ : the even Te and Xe isotopes	Th. Kröll, G. Simpson
IS549	Coulomb Excitation of Neutron-rich $^{134,136}\text{Sn}$ isotopes	Th. Kröll, G. Simpson
IS550	Study of the Dinuclear System $^A\text{Rb} + ^{209}\text{Bi}$ ( $Z1 + Z2 = 120$ )	S. Heinz, E. Kozulin
IS551	Coulomb excitation of doubly magic $^{132}\text{Sn}$ with MINIBALL at HIE-ISOLDE	P. Reiter
IS552	Measurements of octupole collectivity in Rn and Ra nuclei using Coulomb excitation	P.A. Butler, D.T. Joss, M. Scheck
IS553	Determination of the $B(E3, 0^+ \rightarrow 3^-)$ strength in the octupole correlated nuclei $^{142,144}\text{Ba}$ using Coulomb excitation	M. Scheck, D.T. Joss
IS554	Search for higher excited states of $^8\text{Be}^*$ to study the cosmological $^7\text{Li}$ problem	D. Gupta
IS555	Study of shell evolution in the Ni isotopes via one-neutron transfer reaction in $^{70}\text{Ni}$	J.J. Valiente Dobon, R. Orlandi, D. Mengoni
IS556	Spectroscopy of low-lying single-particle states in $^{81}\text{Zn}$ populated in the $^{80}\text{Zn}(d, p)$ reaction	R. Orlandi, R. Raabe
IS557	Coulomb excitation $^{74}\text{Zn}$ - $^{80}\text{Zn}$ ( $N = 50$ ): probing the validity of shell-model descriptions around $^{78}\text{Ni}$	E. Rapisarda, P. Van Duppen, M. Zielinska
IS558	Shape Transition and Coexistence in Neutron-Deficient Rare Earth Isotopes	A. Görgen
IS559	Statistical properties of warm nuclei: Investigating the low-energy enhancement in the gamma strength function of neutron-rich nuclei	S. Siem, M. Wiedeking
IS560	Nuclear-moment studies in the odd-mass In isotopes up to $N = 82$ using the Tilted Foils technique	G. Georgiev
IS561	Transfer reactions at the neutron dripline with triton target	K. Riisager, D. Mücher
IS562	Transfer Reactions and Multiple Coulomb Excitation in the $^{100}\text{Sn}$ Region	J. Cederkäll
IS563	Coulomb excitation of $^{182-184}\text{Hg}$ : Shape coexistence in the neutron-deficient lead region	K. Wrzosek-Lipska, D.T. Joss, D. Jenkins, J. Pakarinen
IS564	Study of the unbound proton-rich nucleus $^{21}\text{Al}$ with resonance elastic and inelastic scattering using an active target	B. Fernández-Dominguez, O. Tengblad, M. Caamano
IS566	Probing intruder configurations in $^{186,188}\text{Pb}$ using Coulomb excitation	J. Pakarinen
IS569	Solving the shape conundrum in $^{70}\text{Se}$	N. Orce, D. Jenkins
IS572	Study of shell evolution around the doubly magic $^{208}\text{Pb}$ via a multinucleon transfer reaction with an unstable beam	J.J. Valiente Dobon, S. Szilner
IS581	Determination of the fission barrier height in fission of heavy radioactive beams induced by the $(d, p)$ -transfer	M. Veselsky, R. Raabe
IS587	Characterising excited states in and around the semi-magic nucleus $^{68}\text{Ni}$ using Coulomb excitation and one-neutron transfer	L. Gaffney, F. Flavigny, M. Zielinska, K. Kolos
IS591	$^{18}\text{N}$ : a challenge to the shell model and a part of the flow path to r-process element production in Type II supernovae	W. Catford, A. Matta
IS595	Spectroscopy of particle-phonon coupled states in $^{133}\text{Sb}$ by the cluster transfer reaction of $^{132}\text{Sn}$ on $^7\text{Li}$ : an advanced test of nuclear interactions	S. Leoni, B. Fornal
IS596	2+ Anomaly and Configurational Isospin Polarization of $^{136}\text{Te}$	V. Werner, N. Pietralla, G. Rainovski
IS597	Probing Shape Coexistence in neutron-deficient $^{72}\text{Se}$ via Low-Energy Coulomb Excitation	D.T. Doherty, J. Ljungvall
IS606	Studies of unbound states in isotopes at the $N = 8$ shell closure	J.G. Johansen
IS607	The $^{59}\text{Cu}(p, \alpha)$ cross section and its implications for nucleosynthesis in core collapse supernovae	C. Lederer
IS616	Reaction mechanisms in collisions induced by $^8\text{B}$ beam close to the barrier	A. Di Pietro, P.-P. Figuera
I150	Shape coexistence in $^{68}\text{Ni}$ and $^{70}\text{Ni}$	F. Recchia, S. Lenzi
I151	Implementing the recoil distance Doppler-shift technique at HIE-ISOLDE: Investigation of neutron-rich $^{86}\text{Se}$	C. Fransen
I152	Shape co-existence and higher order deformations	B.S. Nara Singh, D. Jenkins

degrees of freedom. We therefore divide the discussion below according to the main type of reaction the experiments look for. One of the challenges, and charms, of nuclear physics is that nuclei exhibit many different degrees of freedom. The most important distinction is between single particle and collective degrees of freedom, but the fact that nuclei are composed of two different types of fermions (alternatively: carry also the isospin degree of freedom) adds considerably to the richness of the phenomena observed.

Having access to radioactive beams means we can experimentally vary the neutron and proton numbers  $N$  and  $Z$ . One may distinguish two aspects of how this influences the reactions. First, as  $N$  (or  $Z$ ) is varied neutron (or proton) orbits are filled or emptied, thereby changing the nuclear structure. (Incidentally, we may in some cases —where isomers are present— have several beams with different structures for the same  $N$ ,  $Z$ ; already at REX-ISOLDE experiments have taken place with isomeric beams [74].) The evolution of shell structure [75, 76] or of nuclear shapes [77] are but two of the phenomena that can be studied in this way. Secondly, when the nucleon numbers vary the Fermi levels of neutrons and protons also change. An increased difference between the two Fermi levels clearly influences the reaction dynamics by changing the  $Q$ -values, but structural changes are also well established when the neutron Fermi level reaches the binding threshold, *e.g.* the emergence of halo structures [78–82]. There are predictions that general structure changes may appear also earlier for very neutron-rich systems [83] where the neutron surface could become very diffuse, but the relevant experimental information is still lacking.

#### 4.1.1 Coulomb excitation

Even with state-of-the-art detector arrays and at the radioactive-beam facilities with highest yields one is often only sensitive experimentally to the processes with highest cross-section. For beam energies in the MeV/u range an obvious first choice is Coulomb excitation that can give interesting physics with beam intensities of  $10^4$  ions/s, or even lower. When performed at “safe” energies below the Coulomb barrier one can extract not only excitation energies and suggested spin-assignments from the observed gamma rays, but also information on the matrix elements for transitions among these lowest observed states. Collective degrees of freedom, in particular deformation, are therefore seen very clearly, but the evolution, *e.g.*, along an isotopic chain can also give very direct information on the underlying shell structure. The low-lying spectrum of even-even nuclei is typically easier to interpret, the main feature being a  $0^+ \rightarrow 2^+$  transition from the ground state. The access to the population of the  $4^+$  states will allow for a theory independent verification of the degree of deformation through the  $E_{4^+}/E_{2^+}$  ratio.

Close to the driplines even low-lying excited states will be situated in the continuum and Coulomb excitation will then instead lead to the break-up of the nucleus. The effect this has on the elastic scattering will be discussed below. Coulomb-induced break-up has been employed at higher

beam energy during the last decades as a tool to study the most exotic nuclei [84], in particular the electric dipole response, but the potential for such reactions at a few MeV/u has only been probed sporadically.

Coulomb excitation of the heavy Mg isotopes close to  $N = 20$  was the original motivation when REX-ISOLDE was put forward and several experiments in that region have been carried out. Coulomb excitation of  $^{30}\text{Mg}$  confirmed [85] its spherical shape, whereas for  $^{31}\text{Mg}$  [86] not only the ground state but also excited states were shown to be deformed. Other experiments at ISOLDE have also contributed to unravelling the extent of the island of inversion. The interest in the Mg chain has recently been renewed since it has been shown that the  $N = 20$  and  $N = 28$  islands of inversion are merged [87, 88].

Among the many other examples of results from REX one could mention the studies of evolution of shell structure in the chain of isotopes out to  $^{80}\text{Zn}$  [89] and in the light  $^{106,108,110}\text{Sn}$  nuclei [90]. Two prominent examples of studies of shape evolution (both in heavy nuclei) are that of the shape coexistence in  $^{182-188}\text{Hg}$  [91] and the octupole deformations in Rn and Ra nuclei [13]. More complete overviews of results from REX-ISOLDE and Miniball can be found in [10, 61, 92].

The higher beam energies at HIE-ISOLDE will improve conditions for Coulomb excitation significantly, although one will not be able to employ the highest beam energies if one wants to remain safely below the Coulomb barrier. One-step excitation can take place to higher excitation energies, and multi-step processes become more important and expand the number of transition matrix elements that can be extracted. The detailed analysis often takes place with the GOSIA code [93] and includes the possibility of re-orientation in excited states whereby quadrupole moments may be extracted for excited states. One such case is  $^{70}\text{Se}$  that is the subject of IS569, aiming to settle the shape of the nucleus by combining the Coulex measurement with recent half-life data of the excited state; this is a refinement of an earlier experiment [94] employing the same technique that took place at REX. The improvements of conditions and of the range of the Coulomb excitation method is so that quite a few approved experiments are extensions of the earlier program mentioned above, including IS552, IS557, IS562 and IS563.

Among the many other experiments in this group one can mention a series of attempts to unravel the structure around  $^{132}\text{Sn}$ . The doubly magic nucleus itself with its significantly higher energy for the  $2^+$  state would be studied in IS551 and the evolution beyond  $N = 82$  in  $^{134,136}\text{Sn}$  will be followed in IS549. Adding also a pair of protons, as in  $^{136}\text{Te}$ , gives the possibility of having  $2^+$  states based on both protons and neutrons, and the exact configurations of the lowest two  $2^+$  states (full symmetry, mixed symmetry, proton or neutron dominance, see [95]) will be determined in IS596. Going further up in mass to  $^{142,144}\text{Ba}$  sizeable octupole correlations are expected [96]. Experiment IS553 aims to determine the  $E3$  matrix element for the transition between the ground state and the lowest  $3^-$  state, but needs to employ several targets in order to get suffi-

cient information on the possible Coulomb excitation one-step and multi-step paths. Crossing the  $N = 82$  shell to the region around the neutron-deficient rare-earth nuclei  $^{140}\text{Sm}$  and  $^{142}\text{Gd}$  oblate shapes are expected to lie at low excitation energy. This can be tested directly in Coulomb excitation via the re-orientation effect and is the aim of experiment IS558.

Another region of the nuclear chart where HIE-ISOLDE may be expected to have a high impact is the heavier nuclei where radioactive beams are currently only available at few facilities. One of the highlighted regions for shape coexistence [77] is the neutron-deficient Hg and Pb nuclei where experiments IS563 and IS566 will probe the structure around the mid-shell neutron number  $N = 104$ . The recently installed electron spectrometer SPEDE mentioned in sect. 3.4 will be crucial in both cases and allow to look for the important E0 transition between the two lowest  $0^+$  in the even-even nuclei. At the magic number  $N = 126$  the experiment IS547 will study  $^{206}\text{Hg}$  through single-step and multi-step Coulomb excitation and test the theoretical understanding of this nucleus where rather little is known on the level scheme.

An important addition to the experimental capabilities would be the installation of a plunger, as already implemented at several other laboratories, in particular by the Cologne group. This would allow to measure lifetimes of excited nuclear states in the picosecond range. Letter of intent I151 intends to perform this development and test the method on  $^{86}\text{Se}$  situated just above  $N = 50$ .

#### 4.1.2 One-nucleon transfer reactions

One-nucleon transfer favours transitions corresponding to single-particle degrees of freedom and are very useful for unravelling evolution of shell structure. One typically needs beam intensities around  $10^5$  ions/s to obtain good results with set-ups that include detection of outgoing charged light particles as well as gamma rays from deexcitation of the outgoing nuclei. From the energy and angular distribution of the light particles one can deduce excitation energies of populated levels and restrict their spins and parities. The strength of the transition can be related to the overlap between initial and final state, expressed as a spectroscopic factor (SF) or an asymptotic normalisation constant (ANC). Recent reviews give details on the general theoretical treatment of (d, p) reactions [97] and a selection of results obtained so far with radioactive beams [98,99].

The relative merits of SFs and ANCs have been discussed repeatedly during the last decade, also in connection with nucleon knockout reactions at higher beam energy [100]. An important point has been whether there is a general quenching of SFs similar to what is known to happen in (e, e'p) reactions [101] due to short-range correlations between nucleons, some authors finding that the cross-section in (d, p) reactions for stable nuclei is quenched by a factor 0.55 [102]. A recent overview of this field and on how the overlap functions can be used is pro-

vided in [103] and a compilation of SFs and ANCs for 0p-shell nuclei is given in [104].

The restriction of the energy range at REX-ISOLDE to at most 3.1 MeV/u has so far confined transfer experiments to the lighter isotopes. A series of experiments have been carried out with  $^8\text{Li}$  and  $^{11}\text{Be}$  beams investigating the structure changes in light nuclei close to the neutron dripline [105–107], the  $^{30}\text{Mg}$  beam has been used for (d, p) as well as (t, p) reactions [108], and a  $^{66}\text{Ni}(d, p)$  experiment [109] has started to investigate how the single-particle strength in the neutron orbitals evolves through the neutron-rich Ni-isotopes.

For nuclei close to stability the optimum reaction energy is closer to 10 MeV/u, the angular distributions are easier interpreted here, see [110,111] for a more detailed discussion. The maximum cross-section is likely to be at lower beam energy for very unstable nuclei [112], but angular distributions may not be that easy to unravel. However, this is partly due to the fact that transitions often involve transfer to continuum that is more difficult to treat theoretically, see *e.g.* [113].

There were HIE-ISOLDE letters of intent put forward for transfer experiments in several regions of the nuclear chart, but the proposals have so far focussed on a few regions, the main one being the neutron-rich Ni isotopes. The mapping of the single-particle strength in these nuclei will be improved, making use of the higher reaction energy, in IS587 for  $^{68}\text{Ni}(d, p)$  and continued in IS555 with the  $^{70}\text{Ni}(d, p)$  reaction. Related to these efforts is experiment IS556 that will study the neutron single-particle orbits above  $N = 50$  through the  $^{80}\text{Zn}(d, p)$  reaction. In a separate line of investigation the (d, p) reaction will be used to induce fission in heavy radioactive beams and thereby determine the fission barrier height, this experiment (IS581) would make use of the active target ACTAR.

The proposed spectrometers mentioned in sect. 3.4 would enhance the possibilities for future transfer experiments.

#### 4.1.3 Other reactions

The next step after one-nucleon transfer is to consider two-nucleon transfer, *e.g.* the (t, p) reaction as already employed successfully at REX-ISOLDE to identify the excited  $0^+$  level in  $^{32}\text{Mg}$  [108]. Taking advantage of the increase in beam energy and employing the same tritium target technique, two HIE-ISOLDE experiments (IS561 and IS606) plan to use  $^9\text{Li}$  and  $^{11}\text{Be}$  beams to investigate unbound states at the neutron dripline, namely excited states just above the two-neutron threshold in  $^{11}\text{Li}$  and the levels in the unbound nucleus  $^{13}\text{Be}$ .

Continuing to even heavier targets multi-nucleon transfer becomes important and allows to access other phenomena [114]. An exploratory experiment with a  $^{98}\text{Rb}/^{98}\text{Sr}$  beam on a  $^7\text{Li}$  target has already been performed at REX [115]. The triton-transfer reaction populates levels at such high excitation energy that several neutrons can be emitted. This mechanism will be used in experiment IS595 with a  $^{132}\text{Sn}$  beam. In this way it

should be able to populate states in  $^{133}\text{Sb}$  that are so far unobserved.

It has proven difficult to produce nuclei “south-east” of  $^{208}\text{Pb}$  with conventional reactions. According to calculations multi-nucleon transfer from a heavy neutron-rich projectile may succeed, as it will be attempted by experiment IS572, with an accelerated  $^{94}\text{Rb}$  beam on a  $^{208}\text{Pb}$  target. This method should populate nuclei such as  $^{210}\text{Hg}$  where the current experimental data present puzzles for shell-model calculations.

Elastic scattering reactions may also give interesting information on exotic nuclei [116]. In particular halo nuclei can give a different response from the standard one, as has been elucidated in several experiments carried out at several laboratories including a comprehensive comparison [117] from REX-ISOLDE of elastic scattering of  $^{11}\text{Be}$  on a Zn target with that of  $^{9,10}\text{Be}$  at the same c.m. energy. Due to the coupling to continuum states the low-energy elastic scattering is strongly affected, see *e.g.* [118]. Proceeding further to unbound states, one elegant way of probing them is elastic resonance scattering. The experiment IS564 aims to employ this technique to study the proton-unbound nucleus  $^{21}\text{Al}$  making use of the active target MAYA.

A special group of reactions are the ones motivated in nuclear astrophysics [119]. Although often making use of techniques mentioned earlier they typically need to extract detailed information on specific reactions that can be accessed directly or indirectly. This is illustrated by the experiments IS554 and IS591 that both employ (d, p) transfer reactions. The former is motivated in the  $^7\text{Li}$  abundance anomaly in cosmology where better knowledge on the  $^7\text{Be}$  reaction rates is needed. The latter uses the (d, p) reaction to characterise the levels just above the neutron threshold in  $^{18}\text{N}$ , the properties of which are needed in order to deduce the  $^{17}\text{N}(n, \gamma)$  rate that could be relevant for the r-process in neutrino-driven winds. A different case is provided by the  $^{59}\text{Cu}(p, \alpha)$  reaction that will be studied from 3.6 MeV/u to 5 MeV/u by IS607. This reaction plays a key role in the  $\nu\text{p}$ -process in core collapse supernovae and its rate is crucial in determining whether the process may produce sufficient amounts of the lighter p-nuclei such as  $^{92,94}\text{Mo}$  whose abundance remains a problem. The reaction is furthermore one of the few cases where the reaction rate is needed at high temperatures so that a direct measurement is possible at the energies of interest.

Astrophysics is also part of the motivation for IS559 where inelastic excitations of a pure  $^{66}\text{Ni}$  beam will be detected and analysed within two different frameworks in order to extract the gamma-ray strength function. There are indications that this is enhanced at low energy for stable nearby nuclei, see [120] and references therein, and if a similar enhancement also is present for the neutron-rich nuclei it will obviously affect neutron capture cross-sections.

There are of course more possibilities appearing as the beam energy is increased further, most of these are still unexplored for HIE-ISOLDE. Other laboratories have looked at the peculiarities of fusion reactions including weakly

bound nuclei, a recent review is given in [121]. More complex reactions will occur for heavier radioactive beams on heavy targets above the Coulomb barrier, such as deep inelastic scattering. The proposal that so far goes furthest in this direction is IS550 that aims to explore the physics of super-heavy nuclei through quasi-fission, bombarding a Bi target with the neutron-rich  $^{95}\text{Rb}$ . The cross-sections for quasi-fission are many orders of magnitude above those for fusion and analysis of the reaction products, measured with the CORSET spectrometer, may allow to pinpoint the location of the next magic numbers in the very heavy systems.

## 4.2 Other accelerated beam experiments

Nuclear decays —beta decays, particle decays or the combination beta-delayed particle decays— are sensitive to the nuclear structure and can be very powerful tools to study nuclei far from stability [122–124]. The most spectacular physics is often found in transitions of small branching ratio so that detectors with considerable discrimination ability are needed, one example being the OTPC [68] mentioned in sect. 3.4. Here the radioactive nuclei are implanted deeply into the detector, which requires acceleration to several MeV/u. This technique was used initially at in-flight facilities, but has already been used successfully at REX-ISOLDE for the decay of  $^6\text{He}$  [125]. Implantation into Si-detectors is also an option and have been used to study the beta-delayed  $\alpha$ -decay of  $^{11}\text{Be}$  [126]. The energy increase will allow to extend these method to heavier nuclei where the energy loss in the entrance window is larger.

We note in passing that deep implantations of radioactive ions will be an interesting technique for several solid-state applications.

There are also several techniques that can be applied for measuring the magnetic moments of excited states. One of them is the transient field technique that has already been employed at REX-ISOLDE for the  $2^+$  level of  $^{72}\text{Zn}$  [127] and is proposed in a letter of intent to be used further in the region above  $^{132}\text{Sn}$ . Among the other methods discussed in [17] one makes use of the nuclear alignment that is induced in (multi-nucleon) transfer reactions in order to measure the moments of short-lived isomeric states. Multinucleon transfer gives rise to larger alignment than one-nucleon transfer so HIE-ISOLDE energies are clearly favoured.

The tilted foils polarization technique mentioned in sect. 3.4 is the basis for experiment IS560 where the method will be developed for In beams in order to measure the magnetic moment of the ground states of  $^{129,131}\text{In}$ . This will indicate how robust the  $N = 82$  shell closure is.

## 4.3 Low-energy beams

As discussed in sect. 3.3 the low-energy radioactive-beam experiments at ISOLDE (employing ion beams with energy up to 60 keV or stopped samples) already have benefited from the improvements in beam purity and intensity

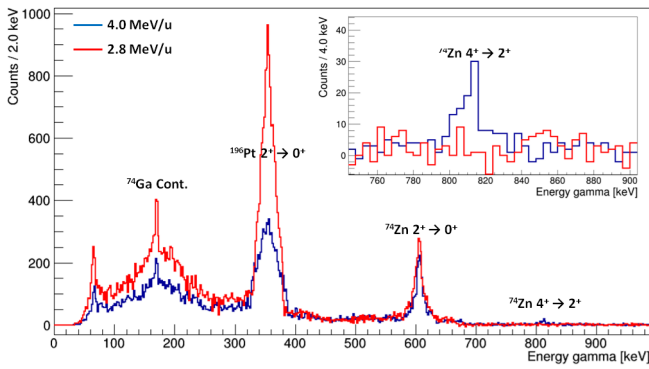


**Fig. 19.** Gamma-ray spectrum of  $^{74}\text{Zn}$ , Coulomb excited at two beam energies: 4 MeV/A beam on  $^{208}\text{Pb}$  target (blue line) and 2.85 MeV/A beam on  $^{196}\text{Pt}$  target (red line). Only a small part of the data has been taken into account. Population of higher-lying states is clearly enhanced at increased beam energy. Courtesy of A. Illana.

that resulted from the major upgrade of the RILIS facility and the installation of the ion beam cooler and buncher ISCOOL.

Very direct examples of the benefits can be found among the many laser experiments that are an important part of the experimental programme at ISOLDE as well as many other radioactive-beam facilities [128–130]. The RILIS improvements have resulted in many new ionization schemes being developed, one spectacular example being the element astatine where the first ionization potential was measured [131]. The use of ISCOOL allows a very significant reduction of background in collinear beam laser spectroscopy experiments as was already apparent from the first tests [132]. It is now an integral and essential part of the experiment CRIS (collinear resonance ionization spectroscopy) [133].

#### 4.4 The first physics output

The first physics experiment to run after installation of the first cryomodule at HIE-ISOLDE was IS557, performing Coulomb excitation of the neutron-rich Zn isotopes. The subtle shell closure at  $N = 40$  mainly observed in the spherical nucleus  $^{68}\text{Ni}$  is presently understood as due to the interplay between the intruder  $1g_{9/2}$  and  $2d_{5/2}$  neutron orbital that induces collectivity by pair excitations from the  $fp$  shell into the  $g_{9/2}$  orbital, and the change in parity that hinders quadrupole excitations. Adding valence nucleons to the  $N = 40$  open shell leads to a rapid increase of collectivity. To learn about the interplay between single particle and collective degrees of freedom one should study in detail this region as these rapid changes indicate underlying complex effects. These phenomena make this region ideal for testing theoretical calculations. In this context the Coulomb excitation study of  $^{74,76}\text{Zn}$  at 4 MeV/u, ideal energy for safe coulex, were chosen as the first HIE-ISOLDE radioactive-beam experiment. The aim was to study the properties of the excited states beyond the  $2^+_1$  state. Of particular interest was the determination of the

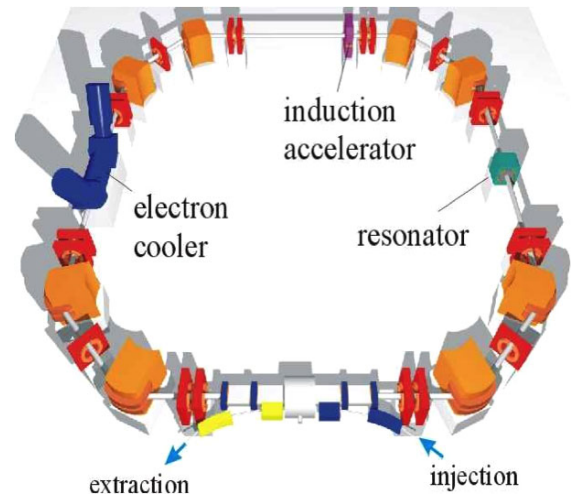


**Fig. 20.** The TSR storage ring from MPI, Heidelberg would add unique experimental possibilities to HIE-ISOLDE. The accelerated beams will be injected into the ring and cooled. Experiments can take place on the circulating beam or by extracting the beam after cooling. Note the possibility of accelerating or decelerating the beam in the ring.

lifetime of the first  $4^+$  state, for which the results of earlier measurements [134,135] were contradictory. Physics runs on  $^{74}\text{Zn}$  and  $^{76}\text{Zn}$  took place in October/November 2015 both at the original REX-ISOLDE energy of 2.85 MeV/u and after acceleration in the superconducting linac to 4 MeV/u, details were given in sect. 3.2.2. The intensities of laser ionised  $^{74,76}\text{Zn}$  beams at the target position were  $10^6$  and  $5 \times 10^5$  pps, respectively. At the latter energy the  $4^+ \rightarrow 2^+$  transition in  $^{74}\text{Zn}$  was clearly enhanced compared to the REX-ISOLDE energy, so a good determination of the lifetime of the  $4^+$  state will be achieved [136]. Figure 19 presents a comparison of  $\gamma$ -ray spectrum for  $^{74}\text{Zn}$  at two beam energies. A clear enhancement of multi-step Coulomb excitation at increased beam energy is observed, demonstrating the new experimental opportunities that open thanks to HIE-ISOLDE.

## 5 Outlook

REX-ISOLDE has since the turn of the century enlarged the physics reach of ISOLDE greatly by adding the possibility of performing nuclear reactions with the large number of radioactive isotopes that can be produced. The main type of reaction studies performed so far are Coulomb excitation due to the upper limit on the reaction energy of 3 MeV/u. By increasing this upper limit to now 5.5 MeV/u and in the near future up to 10 MeV/u, HIE-ISOLDE will drastically increase the possible number of studies that can be performed. This timely increase allows precision nuclear structure studies to be extended to large regions of the nuclear chart that are so far insufficiently explored. This is perfectly aligned with the requirements for future progress in nuclear structure physics as outlined, *e.g.*, in the latest overviews of the field by NSAC [137] and NuPECC [138]. Furthermore, the simultaneous improve-

ments in beam quality and intensity are significant and will benefit much of the physics programme at ISOLDE.

Even though HIE-ISOLDE has only just started to deliver the first of its long awaited physics results, projects to enlarge the capabilities of the facility even further are already quite advanced. The most far-reaching is the installation of a storage-ring by moving the existing TSR from the Max-Planck Institute for Nuclear Physics in Heidelberg to CERN, see fig. 20. A technical design report [139] has identified all requirements for the project and funding for most parts is identified, the main unresolved issue being the construction of a building to house the storage-ring. The new physics possibilities cover a wide range within atomic physics, nuclear physics and nuclear astrophysics [139–141] and involve experiments taking place inside the ring as well as experiments with extracted beams that benefit from the improved beam properties.

ISOLDE has for more than a decade, along with several other European facilities including GANIL, GSI, LNL and Jyväskylä, been involved in the work towards EURISOL. There is still much work to be done before this ambitious high-intensity ISOL facility will be realised, but many of the technical challenges are being addressed through the steady progress accumulated in the existing facilities. The results obtained in the HIE-ISOLDE project will also be an important step towards EURISOL. This synergy is of course clear for the people working on the many aspects of ISOL technology, but it is also being acknowledged on a more official level through the EURISOL-DF (Distributed Facility) collaboration [142].

There are no indications yet that the experimental exploration of nuclei away from beta-stability will be superseded by sufficiently detailed and reliable theoretical calculations. Theory is of course essential for obtaining a full understanding of how nucleons organise themselves in nuclei, but experimental data coming from an increasing number of radioactive beams are clearly needed in the foreseeable future. The ISOLDE facility, as now strengthened through the HIE-ISOLDE project, can contribute in a significant way to this exploration. The facility has a bright and busy future ahead.

A successful project such as HIE-ISOLDE has many proud parents, we would like to thank them all for their efforts during the last decade. We would like to give special thanks to M. Lindroos and P. Butler who started the dream of HIE-ISOLDE, and to Fonds Wetenschappelijk Onderzoek, FWO, Big Science 1 (BE) that on the initiative of M. Huyse, believed in the project and provided the first investments. Special thanks to CERN and the ISOLDE Collaboration, without their support this project will have not been realised. Particular thanks are due to the project leader Y. Kadi and his deputy W. Venturini Delsolaro. We would like also to thank R. Catherall, J. A. Rodriguez and F. Wenander for their comments.

**Open Refereeing** Upon invitation by the communicating editor, referees and authors of this article have agreed to release the original, unedited material of the refereeing procedure for the benefit of the reader. This material is contained in the electronic supplementary material of this article.

## References

1. C. Fahlander, B. Jonson (Editors), *Nobel Symposium 152: Physics with Radioactive Beams*, Phys. Scr. T **152** (2013).
2. Y. Blumenfeld, T. Nilsson, P. Van Duppen, Phys. Scr. T **152**, 014023 (2013).
3. *ISOLDE 50th Anniversary Workshop, December 2014*, contributions available at <http://indico.cern.ch/event/334117/>.
4. P.G. Hansen, in *The History of CERN*, edited by J. Krige, Vol. **III** (North-Holland, Amsterdam, 1996) p. 327.
5. D. Forkel-Wirth, G. Bollen (Editors), *ISOLDE – a laboratory portrait*, Hyperfine Interact. **129** (2000).
6. B. Jonson, K. Riisager, *The ISOLDE facility*, Scholarpedia **5**, issue No. 7, 9742 (2010) doi:10.4249/scholarpedia.9742.
7. A. Herlert, Nucl. Phys. News **20**, 5 (2010).
8. D. Habs *et al.*, *Radioactive beam experiments at ISOLDE: Coulomb excitation and neutron transfer reactions of exotic nuclei*, Proposal to the ISOLDE committee (1994) CERN/ISC 94-25 ISC/P68.
9. N. Orr, J. Phys. G **38**, 020301 (2011).
10. P. Van Duppen, K. Riisager, J. Phys. G **38**, 024005 (2011).
11. D. Habs *et al.*, Hyperfine Interact. **129**, 43 (2000).
12. D. Voulot *et al.*, Nucl. Instrum. Methods B **266**, 4103 (2008).
13. L.P. Gaffney *et al.*, Nature **497**, 199 (2013).
14. M. Lindroos *et al.*, Nucl. Instrum. Methods B **266**, 4687 (2008).
15. *Nuclear Physics and Astrophysics at CERN, October 2005*, contributions available at <http://indico.cern.ch/event/422434/>.
16. M. Lindroos, T. Nilsson (Editors), *HIE-ISOLDE: the technical options*, CERN Yellow Report CERN-2006-013 (2006) <http://cds.cern.ch/record/1001782/files/CERN-2006-013.pdf>.
17. K. Riisager, P. Butler, M. Huyse, R. Krücken (Editors), *HIE-ISOLDE: the scientific opportunities*, CERN Yellow Report CERN-2007-008 (2007) <http://cdsweb.cern.ch/record/1078363/files/CERN-2007-008.pdf>.
18. *New Opportunities in the Physics Landscape at CERN, May 2009*, contributions available at <https://indico.cern.ch/event/51128/>.
19. B.A. Marsh *et al.*, Hyperfine Interact. **196**, 129 (2010).
20. V.N. Fedosseev *et al.*, Rev. Sci. Instrum. **83**, 02A903 (2012).
21. F. Ames, J. Cederkall, T. Sieber, F. Wenander (Editors), *The REX-ISOLDE facility: Design and Commissioning Report*, CERN Report CERN-2005-009 (2005) <https://cds.cern.ch/record/895873>.
22. P. Schmidt *et al.*, Nucl. Phys. A **701**, 550c (2002).
23. H. Raimbault-Hartmann *et al.*, Nucl. Instrum. Methods B **216**, 378 (1997).
24. F. Wenander *et al.*, *REXEBIS, the electron beam ion source for the REX-ISOLDE project: Design and simulations*, CERN OPEN-2000-320 (2000).
25. A.O. Nier, T.R. Roberts, Phys. Rev. **81**, 507 (1951).
26. O. Kester *et al.*, Nucl. Instrum. Methods B **204**, 20 (2003).
27. T. Sieber, *Entwicklung von 4-Rod-und IH-Radio Frequenz Quadrupol(RFQ)-Beschleunigern für radioaktive Ionenstrahlen bei REX-ISOLDE und MAFF*, PhD Thesis, LMU München, May 2001.

28. S. Emhofer, *Aufbau und Vermessung der HF-Eigenschaften des REX-ISOLDE-IH-Beschleunigers*, Diploma Thesis, LMU München, December 1999.
29. H. Podlech *et al.*, *Proceedings of the Seventh European Particle Accelerator Conference, Vienna, 2000* (EPS, Geneva, 2000) p. 572.
30. K.U. Kühnel, Diploma Thesis, IAP Frankfurt, 1999.
31. U. Ratzinger, N. Angert, J. Klabunde, GSI Scientific Report, 1987.
32. D. Warner *et al.*, CERN Heavy-Ion Facility Design Report, CERN 93-01.
33. R. von Hahn *et al.*, Nucl. Instrum. Methods A **328**, 270 (1993).
34. O. Kester, *Proceedings of the Eighth European Particle Accelerator Conference, Paris, 2002* (EPS, Geneva, 2002) p. 915.
35. R. Catherall *et al.*, *HIE-ISOLDE Design Study*, in preparation.
36. M.J.G. Borge *et al.*, JPS Conf. Proc. **6**, 030109 (2015).
37. Y. Kadi, Y. Blumenfeld, R. Catherall, W. Delsolaro Venturini, M.J.G. Borge, *HIE-ISOLDE: The future of radioactive beam physics at CERN*, in press.
38. M.J.G. Borge, Nucl. Instrum. Methods B **376**, 408 (2016).
39. M.A. Fraser, R.M. Jones, M. Pasini, Phys. Rev. ST Accel. Beams **14**, 020102 (2011).
40. M.A. Fraser, *Beam dynamics studies of the ISOLDE post-accelerator of the high intensity and high energy upgrade*, PhD Thesis, University of Manchester, EuCARD Series, Vol. **3** (2012).
41. C. Benvenuti, N. Circelli, M. Hauer, Appl. Phys. Lett. **45**, 583 (1984).
42. C. Benvenuti *et al.*, *Conference Record of the IEEE Particle Accelerator Conference, PAC1991*, Vol. **2** (IEEE, 1991) p. 1023.
43. W. Venturini Delsolaro *et al.*, *Nb sputtered Quarter Wave Resonators for HIE ISOLDE*, in *Proceedings of SRF 2013, Paris, France*, <http://accelconf.web.cern.ch/AccelConf/SRF2013/papers/weioa03.pdf>.
44. J.A. Rodriguez *et al.*, *First operational experience of HIE-ISOLDE*, in *Proceedings of IPAC'16*, available at [www.jacow.org](http://www.jacow.org).
45. F. Zocca *et al.*, Nucl. Instrum. Methods A **672**, 21 (2012).
46. <https://europeanspallationsource.se>.
47. Y. Blumenfeld, P. Butler, J. Cornell, G. Fortuna, M. Lindroos, Int. J. Mod. Phys. E **18**, 1960 (2009).
48. Linac4 Technical Design Report, CERN-AB-2006-084 ABP/RF (2006).
49. M. Vretenar *et al.*, *Status and Plans for LINAC4 installation and commissioning*, in *Proceedings of IPAC'14, Dresden Germany*, ISBN 978-3-95450-132-8, <http://accelconf.web.cern.ch/accelconf/IPAC2014/papers/thpme048.pdf>.
50. G. Arduini *et al.*, *Proceedings of the Chamonix 2010 Workshop on LHC performance*, CERN-ATS-2010-026 228 (2010).
51. R. Garoby *et al.*, *Plans for the upgrade of the LHC injectors*, IPAC2012 Conf. Proc. **C1205201**, TUXA02 (2012) (see <http://www.jacow.org>).
52. J. Coupard *et al.* (Editors), *LHC Injectors Upgrade, TDR, Vol. I: protons*, CERN Accelerator Report, CERN-ACC-2014-0337 (2014).
53. J.-J. Gaimard *et al.*, Nucl. Phys. A **351**, 70 (1991).
54. A. Ferrari, P.R. Sala, A. Fasso, J. Ranft, CERN-2005-10, INFN/TC-05/11, SLAC-R-773 (2005).
55. R. Catherall *et al.*, Nucl. Instrum. Methods B **317**, 204 (2013).
56. B.A. Marsh *et al.*, Nucl. Instrum. Methods B **317**, 550 (2013).
57. B.A. Marsh, Rev. Sci. Instrum. **85**, 02B923 (2014).
58. R.N. Wolf *et al.*, Int. J. Mass. Spectrom. **349-350**, 123 (2013).
59. A. Shornikov, A. Pikin, R. Scrivens, F. Wenander, Nucl. Instrum. Methods B **317**, 395 (2013).
60. F.J.C. Wenander, CERN Yellow Report, CERN-2013-007 doi:10.5170/CERN-2013-007.351, p. 351.
61. N. Warr *et al.*, Eur. Phys. J. A **49**, 40 (2013).
62. V. Bildstein *et al.*, Eur. Phys. J. A **48**, 85 (2012).
63. P. Dendooven, AIP Conf. Proc. **831**, 39 (2006).
64. N. Imai *et al.*, Phys. Rev. C **90**, 011302 (2014).
65. S. Beceiro-Novo, T. Ahn, D. Bazin, W. Mittig, Prog. Part. Nucl. Phys. **84**, 124 (2015).
66. C. Demonchy *et al.*, Nucl. Instrum. Methods A **573**, 145 (2007).
67. J. Pancin *et al.*, Nucl. Instrum. Methods A **735**, 532 (2014).
68. K. Miernik *et al.*, Nucl. Instrum. Methods A **581**, 194 (2007).
69. J.C. Lighthall *et al.*, Nucl. Instrum. Methods A **622**, 97 (2010).
70. R. Raabe, private communication.
71. H. Törnqvist *et al.*, Nucl. Instrum. Methods B **317**, 685 (2013).
72. P. Papadakis *et al.*, JPS Conf. Proc. **6**, 030023 (2015).
73. P. Papadakis *et al.*, J. Phys.: Conf. Ser. **312**, 052017 (2011).
74. I. Stefanescu *et al.*, Phys. Rev. Lett. **98**, 122701 (2007).
75. O. Sorlin, M.-G. Porquet, Prog. Part. Nucl. Phys. **61**, 602 (2008).
76. R. Kanungo, Phys. Scr. T **152**, 014002 (2013).
77. K. Heyde, J.L. Wood, Rev. Mod. Phys. **83**, 1467 (2011).
78. B. Jonson, Phys. Rep. **389**, 1 (2004).
79. A.S. Jensen *et al.*, Rev. Mod. Phys. **76**, 215 (2004).
80. I. Tanihata, H. Savajols, R. Kanungo, Prog. Part. Nucl. Phys. **68**, 215 (2013).
81. K. Riisager, Phys. Scr. T **152**, 014001 (2013).
82. L.V. Chulkov, B. Jonson, M.V. Zhukov, Eur. Phys. J. A **51**, 97 (2015).
83. J. Dobaczewski, I. Hamamoto, W. Nazarewicz, J.A. Sheikh, Phys. Rev. Lett. **72**, 981 (1994).
84. T. Auman, T. Nakamura, Phys. Scr. T **152**, 014012 (2013).
85. O. Niedermaier *et al.*, Phys. Rev. Lett. **94**, 172501 (2005).
86. M. Seidlitz *et al.*, Phys. Lett. B **700**, 181 (2011).
87. P. Doornenbal *et al.*, Phys. Rev. Lett. **111**, 212502 (2013).
88. E. Caurier, F. Nowacki, A. Poves, Phys. Rev. C **90**, 014302 (2014).
89. J. Van de Walle *et al.*, Phys. Rev. Lett. **99**, 142501 (2007).
90. A. Ekström *et al.*, Phys. Rev. Lett. **101**, 012502 (2008).
91. N. Bree *et al.*, Phys. Rev. Lett. **112**, 162701 (2014).
92. T. Kröll, EPJ Web of Conferences **66**, 02059 (2014).
93. M. Zielińska *et al.*, Eur. Phys. J. A **52**, 99 (2016).
94. A.M. Hurst *et al.*, Phys. Rev. Lett. **98**, 072501 (2007).
95. N. Pietralla, P. von Brentano, A.F. Lisetskiy, Prog. Part. Nucl. Phys. **60**, 225 (2008).
96. B. Bucher *et al.*, Phys. Rev. Lett. **116**, 112503 (2016).

97. R.C. Johnson, *J. Phys. G* **41**, 094005 (2014).
98. K.L. Jones, *Phys. Scr. T* **152**, 014020 (2013).
99. V. Lapoux, N. Alamanos, *Eur. Phys. J. A* **51**, 19 (2015).
100. P.G. Hansen, J.A. Tostevin, *Annu. Rev. Nucl. Part. Sci.* **53**, 219 (2003).
101. V.R. Pandharipande, I. Sick, P.K.A. deWitt Huberts, *Rev. Mod. Phys.* **69**, 981 (1997).
102. B.P. Kay, J.P. Schiffer, S.J. Freeman, *Phys. Rev. Lett.* **111**, 042502 (2013).
103. N.K. Timofeyuk, *J. Phys. G* **41**, 094008 (2014).
104. N.K. Timofeyuk, *Phys. Rev. C* **88**, 044315 (2013).
105. H.B. Jeppesen *et al.*, *Phys. Lett. B* **642**, 449 (2006).
106. E. Tengborn *et al.*, *Phys. Rev. C* **84**, 064616 (2011).
107. J.G. Johansen *et al.*, *Phys. Rev. C* **88**, 044619 (2013).
108. K. Wimmer *et al.*, *Phys. Rev. Lett.* **105**, 252501 (2010).
109. J. Diriken *et al.*, *Phys. Lett. B* **736**, 533 (2014).
110. J.S. Winfield, W.N. Catford, N.A. Orr, *Nucl. Instrum. Methods A* **396**, 147 (1997).
111. W.N. Catford, *The Euroschool on Exotic Beams*, Vol. **IV** (Springer, 2014) pp. 67–122.
112. H. Lenske, G. Schrieder, *Eur. Phys. J. A* **2**, 41 (1998).
113. A. Bonaccorso, *Phys. Scr. T* **152**, 014019 (2013).
114. L. Corradi, G. Pollarolo, S. Szilner, *J. Phys. G* **36**, 113101 (2009).
115. S. Bottoni *et al.*, *Acta Phys. Pol. B* **45**, 343 (2014).
116. N. Keeley, N. Alamanos, K.W. Kemper, K. Rusek, *Prog. Part. Nucl. Phys.* **63**, 396 (2009).
117. A. Di Pietro *et al.*, *Phys. Rev. Lett.* **105**, 22701 (2010).
118. A. Diaz-Torres, A.M. Moro, *Phys. Lett. B* **733**, 89 (2014).
119. J. José, C. Iliadis, *Rep. Prog. Phys.* **74**, 096901 (2011).
120. M. Wiedeking *et al.*, *Phys. Rev. Lett.* **108**, 162503 (2012).
121. L.F. Canto, P.R.S. Gomes, R. Donangelo, J. Lubian, M.S. Hussein, *Phys. Rep.* **596**, 1 (2015).
122. B. Blank, M.J.G. Borge, *Prog. Part. Nucl. Phys.* **60**, 403 (2008).
123. M. Pfützner, M. Karny, L. Grigorenko, K. Riisager, *Rev. Mod. Phys.* **84**, 567 (2012).
124. M.J.G. Borge, *Phys. Scr. T* **152**, 014013 (2013).
125. M. Pfützner *et al.*, *Phys. Rev. C* **92**, 014316 (2015).
126. J. Büscher, PhD Thesis, KU Leuven (2010) unpublished.
127. A. Illana *et al.*, *Phys. Rev. C* **89**, 054316 (2014).
128. B. Cheal, K.T. Flanagan, *J. Phys. G* **37**, 113101 (2010).
129. K. Blaum, J. Dilling, W. Nörtershäuser, *Phys. Scr. T* **152**, 014017 (2013).
130. P. Campbell, I.D. Moore, M.R. Pearson, *Prog. Part. Nucl. Phys.* **86**, 127 (2016).
131. S. Rothe *et al.*, *Nature Commun.* **4**, 1835 (2013).
132. E. Mané *et al.*, *Eur. Phys. J. A* **42**, 503 (2009).
133. K. Flanagan, *Nucl. Phys. News* **23**, issue No. 2, 24 (2013).
134. J. Van de Walle *et al.*, *Phys. Rev. C* **79**, 0142309 (2009).
135. C. Louchart *et al.*, *Phys. Rev. C* **87**, 054302 (2013).
136. A. Illana *et al.*, in preparation.
137. *The 2015 NSAC Long Range Plan for Nuclear Science*, available at <http://science.energy.gov/np/nsac/reports/>.
138. *NuPECC Long Range Plan 2010: Perspectives of Nuclear Physics in Europe*, available at <http://nupecc.org>.
139. M. Grieser *et al.*, *Eur. Phys. J. ST* **207**, 1 (2012).
140. P. Butler *et al.*, *Nucl. Instrum. Methods B* **376**, 270 (2016).
141. P. Butler *et al.*, *Acta Phys. Pol. B* **47**, 627 (2016).
142. <http://www.eurisol.org/eurisol-df/>.



María José García Borge completed her studies and her doctorate (1982) at the “Universidad Complutense” of Madrid. She was a “Fulbright-fellow” at the University of Arizona, USA. Afterwards she became a “CERN fellow” where she worked at the ISOLDE facility for more than two years.

Since 1986 she is a member of CSIC where she has created and led a research group dedicated to the study of exotic nuclei, their structure, dynamic and decay modes. With her work she has actively promoted the expansion of experimental nuclear physics in Spain. She has more than two hundred papers published in the most prestigious journals including *Nature*. She has been an organizer of a dozen conferences, member of numerous scientific committees and chair of the ISOLDE Collaboration committee. It is the Spanish representative in the European Expert Committee for Nuclear Physics, NuPECC since 2009 and chair of the Editorial Board of the *Nuclear Physics News* magazine. Currently she is working at CERN as leader and spokesperson of the ISOLDE Facility.



Karsten Riisager obtained a PhD in 1986 and the Dr. Scient. degree in 1994, both from Aarhus University where he is currently employed. He has worked on decay and reaction experiments with radioactive beams at many European facilities, in particular ISOLDE at CERN where he was group leader in 2005–2008. He has served in program advisory boards at CERN, JYFL, GANIL and TRIUMF.